Patients who experience recurrence after LT show rapid progression of recurrent disease and have a very poor prognosis because the rate of progression of recurrent HCC is more rapid after transplantation than after hepatic resection (*11, 12*). However, some patients have a good prognosis if they are appropriately treated after recurrence. Hence, it is important to predict not only who is likely to exhibit recurrence but also who may survive longer. There are no reports about the relationship between NLR and patients with recurrent HCC after LDLT, and there is little information regarding prognosis and treatment for HCC recurrence after LT. Therefore, in this study, we investigated the relationship between preoperative and postoperative NLR and prognosis of patients with recurrent HCC after LDLT.

RESULTS

In total, HCC recurrence was identified in 26 (15.5%) patients: 16 men and 10 women among the 167 patients with HCC. The mean duration until the initial recurrence after LDLT was 3.7 years, and the mean duration until death the initial recurrence was 1.7 years. Clinicopathologic factors on recurrence of HCC after LDLT using univariate analysis are shown in Table 1 and Table S1 (see **SDC**, http://links.lww.com/TP/A868). AFP ≧300 ng/mL, DCP ≧300 mAU/mL, NLR ≧4, tumor number >3, tumor size ≧5 cm, duration of last treatment of HCC to LDLT <3 months, Milan criteria exceeded, histologic tumor number ≧10, histologic tumor size >5 cm, poor differentiation, presence of histologic vascular invasion, adjuvant chemotherapy, and interferon (IFN) therapy against patients with hepatitis C virus (HCV) were significant differences between patients with recurrence and without recurrence of HCC. There were no significant differences regarding host-related factors except IFN between the two groups.

The prognostic factors for survival after recurrence using univariate analysis are shown in Table 2. These data included both factors before LDLT (Table 2) and those after LDLT (Table 3). Male sex, IFN therapy against patients with HCV, AFP ≧300 ng/mL at recurrence, NLR ≧4 at recurrence, and nonsurgical resection for recurrent HCC were significantly related to poor prognosis. The survival curves after recurrence for the patients with NLR ≧4 at recurrence are illustrated in Figure 1. The 3-year survival curves after recurrence were 0% in patients with NLR ≧4 and 43.6% in patients with NLR <4. The 3-year survival curves after recurrence were 50% in females and 9.5% in males, whereas the 3-year survival curves after recurrence were 53.3% in patients with IFN therapy against HCV and 0% in patients without IFN therapy. Furthermore, the 3-year survival curve after recurrence were 0% in patients with AFP ≧300 ng/mL at recurrence and 28.4% in patients with AFP <300 ng/mL. The 3-year survival curves after recurrence were 41.7% in patients with surgical resection for recurrent HCC and 0% in patients without surgical resection for recurrent HCC. Interestingly, AFP and NLR before LDLT, in particular, were not related to survival after recurrence of HCC. Multivariate analysis was not performed because of the small sample size.

NLR was reelevated after LDLT in patients who later died, whereas NLR gradually decreased in surviving patients (Fig. 2).

DISCUSSION

Using univariate analysis, our retrospective study indicated that male sex, IFN therapy for HCV, NLR and AFP at recurrence, and surgical resection for recurrent HCC were poor prognostic factors for survival after recurrence of HCC among patients with LDLT. We recently proposed new selection criteria for LDLT in patients with HCC (*7*). A multivariate analysis identified independent risk factors for post-LDLT tumor recurrence including tumor size, the presence of eight or more tumors, and an NLR of 4 or more. These criteria could effectively exclude patients with biologically

TABLE 1. Patients and tumor characteristics between patients with recurrence and without recurrence of HCC

Factors	Patients with recurrent HCC (n=26)	Patients without recurrent HCC (n=141)	*P*
AFP (ng/mL) <300/≧300	12/14	126/15	0.001
DCP (mAU/mL) <300/≧300	12/14	122/19	0.001
NLR <4/≧4	16/10	125/16	0.001
Number of tumors ≦3/>3	16/10	108/33	0.002
Tumor size (cm) ≦5/>5	6/20	139/2	0.001
Duration of last treatment to LDLT			
<3/≧3 months	16/10	127/14	0.001
Milan criteria, yes/No	7/19	98/43	0.001
Number of tumors (histologic)			
<10/≧10	13/13	114/27	0.002
Tumor size (cm) (histologic)			
≦5/>5	9/17	137/4	0.001
Tumor differentiation (histologic)			
Well+moderate/poor	16/10	111/30	0.001
Vascular invasion (histologic)			
Yes/no	18/8	40/101	0.001
IFN			
Yes/no	8/11	69/30	0.032

TABLE 2. Clinicopathologic factors on survival after recurrence of HCC using univariate analysis

Factors before LDLT	Patients	Survival at 3 years (%)	P
Gender			
Male	16	9.5	0.006
Female	10	50.0	
Age (years)			
≦57	12	13.0	0.943
>57	14	36.5	
Hepatitis			
HCV	19	20.2	0.489
Non-HCV	7	45.7	
Child-Pugh classification			
A+B	14	0	0.066
C	12	44.2	
MELD score			
<15	21	34.2	0.157
≧15	5	0	
AFP (ng/mL)			
<300	14	32.7	0.709
≧300	12	15.6	
DCP (mAU/mL)			
<300	14	35.0	0.185
≧300	12	16.7	
NLR			
<4	16	26.7	0.981
≧4	10	24.2	
Number of tumors			
≦3	10	33.3	0.613
>3	16	25.0	
Tumor size (cm)			
≦5	20	28.4	0.818
>5	6	16.7	
Duration of initial HCC to LDLT			
<1 year	7	16.2	0.509
≧1 year	15	28.6	
Duration of last treatment to LDLT			
<3 months	16	35.4	0.191
≧3 months	10	11.1	
Milan criteria			
Yes	7	60.0	0.481
No	19	21.1	
Graft vs. standard liver volume (%)			
<35	6	29.6	0.976
≧35	20	20.8	
Age of donor (year)			
≦30	11	15.0	0.926
>30	15	36.2	

aggressive tumors before LT, promoting an extremely low recurrence rate.

The rate of HCC recurrence after transplantation has ranged from 8% to 22.7% in different studies (*13–16*). Patients who experience recurrence after LT show rapid progression of recurrent disease and have a very poor prognosis such that median survival after recurrence ranged from 7 to 9 months because the rate of progression of recurrent HCC is more rapid after transplantation than after hepatic resection (*15, 17*). The main reason for this poor outcome is that the progression of the disease is usually fast because of the immunosuppressed state after transplantation. However, some patients have a good prognosis if they are appropriately treated after recurrence. In this study, NLR and AFP at recurrence are useful biomarkers to predict the prognosis after

TABLE 3. Clinicopathologic factors on survival after recurrence of HCC using univariate analysis

Factors after LDLT	Patients	Survival at 3 years (%)	P
Number of tumors (histologic)			
<10	13	42.9	0.102
≧10	13	10.0	
Tumor size (cm) (histologic)			
≦5	17	28.6	0.488
>5	9	22.2	
Tumor differentiation (histologic)			
Well+moderate	10	27.8	0.819
Poor	16	11.5	
Vascular invasion (histologic)			
Yes	18	19.7	0.446
No	8	38.1	
Adjuvant chemotherapy			
Yes	11	27.3	0.630
No	15	25.0	
CNI			
CyA	13	18.2	0.653
Tac	13	32.3	
Steroid use			
Yes	17	14.1	0.134
No	9	42.9	
IFN against HCV			
Yes	9	53.3	0.013
No	11	0	
AFP (ng/mL) at recurrence			
<300	23	28.4	0.001
≧300	3	0	
DCP (mAU/mL) at recurrence			
<300	21	31.4	0.120
≧300	5	0	
NLR at recurrence			
<4	17	43.6	0.006
≧4	9	0	
Initial site of recurrence			
Liver	4	33.3	0.986
Extraliver	22	22.6	
Duration of LDLT to recurrence (years)			
>1	12	40.0	0.097
≧1	14	12.2	
Surgical resection for recurrent HCC			
Yes	14	41.7	0.002
No	12	0	

recurrent HCC. This is the first report to discuss the relationship between NLR and the prognosis in patients with recurrent HCC after LDLT.

It is difficult to treat recurrences because these tumors tend to be involved in multiple organs, and if the tumor recurs in a single organ, it usually manifests multiple lesions. These findings suggest that the aggressiveness of the tumor and the effectiveness of the treatment for the recurrent lesion were important to survival after recurrence. If the recurrent disease progressed slowly and if the recurrent lesion was locally controllable, patient survival could be prolonged. Hence, it is important to predict not only who may live but also who can survive longer after recurrence.

Roayaie et al. (*15*) described that the surgical treatment of recurrence was independently associated with significantly longer survival. Furthermore, several articles suggested that surgical treatment of recurrent tumors after LT should be considered whenever possible (*14–16*). However, the indications for surgical resection of recurrent HCC are a solitary tumor or curative resection; thus, there is possibility that the patient whose recurrence had more malignant behavior (multiple recurrence or multisite recurrence) was eliminated as a candidate of surgical treatment. Interestingly, none of the primary tumor characteristics were associated with survival after HCC recurrence. There was no association of the survival after recurrence such as tumor size, number of tumors, tumor marker at pre-LT, histologic differentiation, or vascular invasion. Schlitt et al. (*16*) also reported that no primary tumor characteristics were associated with survival after HCC recurrence. These findings suggest that the malignant phenotype of the recurrent HCC might be quite different from that of the primary HCC. In our study, a univariate analysis showed that sex, IFN therapy for HCV, AFP ≧300 ng/mL at recurrence, NLR ≧4 at recurrence, and surgical resection were significant factors for recurrent HCC. Tumor growth in recurrent HCC is quicker after LT mainly because of the need for permanent immunosuppression (*17*). NLR and AFP at recurrence may reflect the biological malignant behavior.

The molecular mechanism associated with elevated NLR and the prognosis of patients with HCC is associated

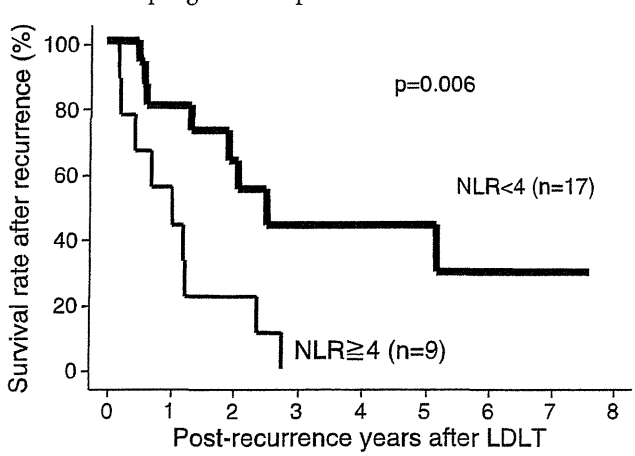

FIGURE 1. Survival after recurrence in patients with NLR<4 at recurrence or those with NLR≧4 at recurrence. Survival after recurrence in patients with NLR≧4 at recurrence was significantly poor prognosis.

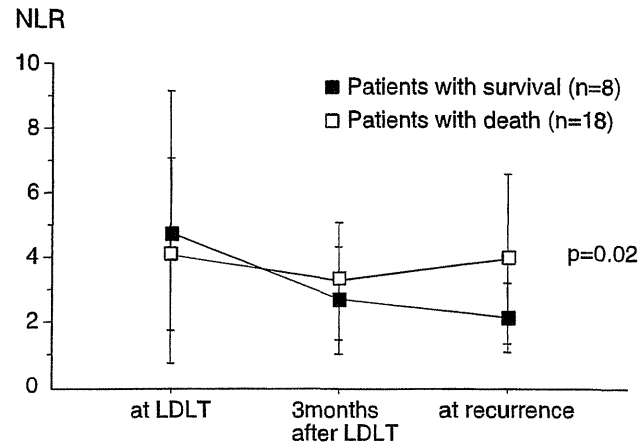

FIGURE 2. Time-dependent NLR at LDLT, 3 months after LDLT, and at recurrence. □, patients with death; ■, patients with survival. NLR was reelevated after LDLT in patients with death; on the contrary, NLR was gradually decreased with patients with survive.

with many factors, but it remains poorly understood. Chronic systemic inflammation is an important prognostic factor in patients with cancer. The NLR was used as a parameter of chronic inflammation in patients with cancer. We previously showed that NLR was an important prognostic factor in patients with HCC after hepatic resection (*9*) and in patients who underwent LDLT (*10*). A close relationship between accumulation of tumor-associated macrophages in HCC and high NLR levels was observed in patients with HCC who underwent hepatic resection and LDLT (*18*). A high NLR is associated with a high infiltration of tumor-associated macrophages and high inflammatory cytokine production in the tumor, such as interleukin-6 and interleukin-8, which promote systemic neutrophilia.

In conclusion, this retrospective analysis revealed that NLR at recurrence is a prognostic factor affecting survival after recurrence in LDLT for HCC. A multi-institutional study is needed to provide evidence of the significance of NLR in HCC.

MATERIALS AND METHODS

Patient Characteristics

A total of 393 LDLT operations were performed at Kyushu University Hospital from October 1996 to August 2012 after approval was obtained from the Ethics and Indications Committee of Kyushu University. Among them, 167 adult-to-adult LDLTs for HCC were enrolled in this study. The selection criteria for the HCC patients were as follows: (a) no modality, except LDLT available to cure patients with HCC and end-stage liver disease; (b) no extrahepatic metastasis; and (c) no major vascular infiltration, such as the portal vein or hepatic vein, thus indicating that there was no restriction on the tumor size or the number of the tumors.

The transplant procedures for both the donors and recipients have been described previously (*6*). The immunosuppressive regimen consisted of the combination of a calcineurin inhibitor (CNI) (tacrolimus [Tac] or cyclosporine A [CyA]) and steroid with or without mycophenolate mofetil. A steroid injection was given intravenously (methylprednisolone 1 g) and tapered to zero by day 7. Mycophenolate mofetil (1 g/day) treatment was started from postoperative day 1 and completed by 3 months. A maintenance immunosuppression therapy was conducted with low-dose Tac or CyA from postoperative day 7. Adjuvant systemic chemotherapy using 5-fluorouracil

and cisplatin with or without gemcitabine for 1 month were administered to patients who had more than 300 mAU/mL DCP, more than 5 cm of maximum tumor size, or who exceeded the Milan criteria.

Prognostic Factor

The prognostic factors were examined with respect to survival after recurrence of HCC based on the following variables: sex (male vs. female), age (≧57 vs. <57 years), hepatitis (HCV vs. non-HCV), Child-Pugh classification (A+B vs. C), the Model for End-Stage Liver Disease (MELD) score (<15 vs. ≧15), serum AFP level (≧300 vs. <300 ng/mL), DCP level (≧300 vs. <300 mAU/L), NLR (≧4.0 vs. <4.0), number of tumors (≦3 vs. >3), tumor size (≦5 vs. >5 cm), duration of initial HCC to LDLT (<1 vs. ≧1 year), duration of last treatment to LDLT (<3 vs. ≧3 months), Milan criteria (yes vs. no), graft vs. standard liver volume (<35% vs. ≧35%), age of donor (<30 vs. >30 years), histologic number of tumors (<10 vs. ≧10), histologic tumor size (≦5 vs. >5 cm), histologic tumor differentiation (well+moderate vs. poor), histologic vascular invasion (yes vs. no), adjuvant chemotherapy (yes vs. no), CNI (CyA vs. Tac), steroid use (yes vs. no), IFN against HCV (yes vs. no), AFP level at recurrence (≧300 vs. <300 ng/mL), DCP level at recurrence (≧300 vs. <300 mAU/L), NLR at recurrence (≧4.0 vs. <4.0), initial site of recurrence (liver vs. extraliver), duration of LDLT to recurrence (<1 vs. ≧1 year), and surgical resection for recurrent HCC (yes vs. no).

Patient Follow-up

The clinical follow-up of patients transplanted for HCC followed a strict protocol, which did not change during the study period. The patients were seen biweekly for the first month and then screened monthly for 6 months for tumor markers such as AFP and DCP. The patients had ultrasound scans and enhanced computed tomography scans at 6-month intervals. When recurrence was suspected, additional examination such as hepatic angiography were performed. The median follow-up period was 3.9 years.

Treatment of HCC Recurrence

Patients with recurrence that could be surgically cured underwent a resection or ablation of their tumors. All patients considered to be unsuitable for surgical treatment were referred for palliative care by radiotherapy, transarterial chemoembolization, and administration of 5-fluorouracil–based systemic therapy.

Histologic Study

All of the resected specimens were cut into serial 5- to 10-mm-thick slices and fixed in 10% formalin. After macroscopic examination, the slice with the greatest dimensions was trimmed for embedding in paraffin and cut into 4-μm microscopic sections. The sections were stained with hematoxylin-eosin. Tumor differentiation, microvascular invasion, intrahepatic metastasis, and histologic liver cirrhosis were examined by the pathologist according to the Liver Cancer Study Group in Japan (*19*).

Statistical Analysis

We analyzed the categorical clinicopathologic variables using the chi-square test or Fisher's exact test. Continuous variables were expressed as means and SDs and compared with the Student's *t* test. The survival curves after recurrence of the two groups were analyzed by the Kaplan–Meier method and compared with the log-rank test. All analyses were performed with Statview 5.0 software (Abacus Concepts, Berkeley, CA). NLR in a subsequent phase were compared by repeated-measures analysis of variance. $P<0.05$ was considered statistically significant.

REFERENCES

1. Llovcet JM, Burroughs A, Bruix J Hepatocellular carcinoma. *Lancet* 2003; 362: 1907.
2. Kiyosawa K, Tanaka E Characteristics of hepatocellular carcinoma in Japan. *Oncology* 2002; 62: 5.
3. Mazzaferro V, Regalia E, Doci R, et al. Liver transplantation for the treatment of small hepatocellular carcinomas in patients with cirrhosis. *N Engl J Med* 1996; 334: 693.
4. Yao FY, Ferrell L, Bass NM, et al. Liver transplantation for hepatocellular carcinoma: expansion of the tumor size limits does not adversely impact survival. *Hepatology* 2001; 33: 1394.
5. Mazzaferro V, Llovet JM, Miceli R, et al. Predicting survival after liver transplantation in patients with hepatocellular carcinoma beyond the Milan criteria: a retrospective, exploratory analysis. *Lancet Oncol* 2009; 10: 35.
6. Taketomi A, Sanefuji K, Soejima Y, et al Impact of des-gamma-carboxy prothrombin and tumor size on the recurrence of hepatocellular carcinoma after living donor liver transplantation. *Transplantation* 2009; 87: 531.
7. Yoshizumi T, Ikegami T, Yoshiya S, et al. Impact of tumor size, number of tumors and neutrophil-to-lymphocyte ratio in liver transplantation for recurrent hepatocellular carcinoma. *Hepatol Res* 2013; 43: 709.
8. Shirabe K, Taketomi A, Morita K, et al. Comparative evaluation of expanded criteria for patients with hepatocellular carcinoma beyond the Milan criteria undergoing living-related donor liver transplantation. *Clin Transplant* 2011; 25: E491.
9. Mano Y, Shirabe K, Yamashita YI, et al. Preoperative neutrophil-to-lymphocyte ratio is a predictor of survival after hepatectomy for hepatocellular carcinoma. A retrospective analysis. *Ann Surg* 2013; 258: 301.
10. Motomura T, Shirabe K, Mano Y, et al. Neutrophil-lymphocyte ratio reflects hepatocellular carcinoma recurrence after liver transplantation via inflammatory microenvironment. *J Hepatol* 2013; 58: 58.
11. Escartin A, Sapisochin G, Bilbao I, et al. Recurrence of hepatocellular carcinoma after liver transplantation. *Transplant Proc* 2007; 39: 2308.
12. Regalia E, Fassati LR, Valente U, et al. Pattern and management of recurrent hepatocellular carcinoma after liver transplantation. *J Hepatobil Pancreat Surg* 1998; 5: 29.
13. Shin WY, Suh KS, Lee HW, et al. Prognostic factors affecting survival after recurrence in adult living donor liver transplantation for hepatocellular carcinoma. *Liver Transpl* 2010; 16: 678.
14. Taketomi A, Fukuhara T, Morita K, et al. Improved results of a surgical resection for the recurrence of hepatocellular carcinoma after living donor liver transplantation. *Ann Surg Oncol* 2010; 17: 2283.
15. Roayaie S, Schwartz JD, Sung MW, et al. Recurrence of hepatocellular carcinoma after liver transplant: patterns and prognosis. *Liver Transpl* 2004; 10: 534.
16. Schlitt HJ, Neipp M, Weimann A, et al. Recurrence patterns of hepatocellular and fibrolamellar carcinoma after liver transplantation. *J Clin Oncol* 1999; 17: 324.
17. Yokoyama I, Carr B, Saitsu H, et al. Accelerated growth rates of recurrent hepatocellular carcinoma after liver transplantation. *Cancer* 1991; 68: 2095.
18. Shirabe K, Mano Y, Muto J, et al. Role of tumor-associated macrophages in the progression of hepatocellular carcinoma. *Surg Today* 2012; 42: 1.
19. Liver Cancer Study Group of Japan. General Rules for the Clinical and Pathological Study of Primary Liver Cancer. Second English edition, pp. 34–35, Kanehara & Co., Tokyo, 2003.

Modulation of the Biliary Expression of Arylalkylamine N-Acetyltransferase Alters the Autocrine Proliferative Responses of Cholangiocytes in Rats

Anastasia Renzi,[3,7] Sharon DeMorrow,[2,3] Paolo Onori,[6] Guido Carpino,[10] Romina Mancinelli,[7] Fanyin Meng,[2,3,4] Julie Venter,[3] Mellanie White,[3] Antonio Franchitto,[7,9] Heather Francis,[2,3,4] Yuyan Han,[3] Yoshiyuki Ueno,[8] Giuseppina Dusio,[4] Kendal J. Jensen,[3] John J. Greene, Jr.,[5] Shannon Glaser,[1,2,3*] Eugenio Gaudio,[7*] and Gianfranco Alpini[1,2,3*]

Secretin stimulates ductal secretion by interacting with secretin receptor (SR) activating cyclic adenosine 3′,5′-monophosphate/cystic fibrosis transmembrane conductance regulator/chloride bicarbonate anion exchanger 2 (cAMP⇒CFTR⇒Cl^-/HCO_3^- AE2) signaling that is elevated by biliary hyperplasia. Cholangiocytes secrete several neuroendocrine factors regulating biliary functions by autocrine mechanisms. Melatonin inhibits biliary growth and secretin-stimulated choleresis in cholestatic bile-duct–ligated (BDL) rats by interaction with melatonin type 1 (MT1) receptor through down-regulation of cAMP-dependent signaling. No data exist regarding the role of melatonin synthesized locally by cholangiocytes in the autocrine regulation of biliary growth and function. In this study, we evaluated the (1) expression of arylalkylamine N-acetyltransferase (AANAT; the rate-limiting enzyme for melatonin synthesis from serotonin) in cholangiocytes and (2) effect of local modulation of biliary AANAT expression on the autocrine proliferative/secretory responses of cholangiocytes. In the liver, cholangiocytes (and, to a lesser extent, BDL hepatocytes) expressed AANAT. AANAT expression and melatonin secretion (1) increased in BDL, compared to normal rats and BDL rats treated with melatonin, and (2) decreased in normal and BDL rats treated with AANAT Vivo-Morpholino, compared to controls. The decrease in AANAT expression, and subsequent lower melatonin secretion by cholangiocytes, was associated with increased biliary proliferation and increased SR, CFTR, and Cl^-/HCO_3^- AE2 expression. Overexpression of AANAT in cholangiocyte cell lines decreased the basal proliferative rate and expression of SR, CFTR, and Cl^-/HCO_3^- AE2 and ablated secretin-stimulated biliary secretion in these cells. *Conclusion*: Local modulation of melatonin synthesis may be important for management of the balance between biliary proliferation/damage that is typical of cholangiopathies. (HEPATOLOGY 2013;57:1130-1141)

Cholangiocytes modify canalicular bile before it reaches the duodenum through a series of secretory/absorptive events regulated by gastrointestinal hormones, including secretin.[1,2] Secretin stimulates bile secretion by interaction with secretin receptor (SR) expressed only by large cholangiocytes in the liver.[3] Binding of secretin to its receptor induces an increase in cyclic adenosine 3′,5′-monophosphate (cAMP) levels,

Abbreviations: AANAT, serotonin N-acetyltransferase or arylalkylamine N-acetyltransferase; ALP, alkaline phosphatase; ASMT, N-acetylserotonin O-methyltransferase; BDL, bile duct ligation; BSA, bovine serum albumin; BW, body weight; cAMP, cyclic adenosine 3′,5′-monophosphate; CFTR, cystic fibrosis transmembrane conductance regulator; CK-19, cytokeratin-19; Cl⁻/HCO3– AE2, chloride bicarbonate anion exchanger 2; ELISA, enzyme-linked immunosorbent assay; FACS, fluorescence-activated cell sorting; GAPDH, glyceraldehyde-3-phosphate dehydrogenase; IBDM, intrahepatic bile duct mass; H&E, hematoxylin and eosin; IHC, immunohistochemistry; MC, mouse cholangiocyte line; MT1, melatonin type 1; mRNA, messenger RNA; NCBI, National Center for Biotechnology Information; OS, oxidative stress; PCNA, proliferating cell nuclear antigen; PCR, polymerase chain reaction; PKA, protein kinase A; SEM, standard error of the mean; SGOT, serum glutamic oxaloacetic transaminase; SGPT, serum glutamate pyruvate transaminases; SR, secretin receptor; TBIL, total bilirubin; VEGF-A/C, vascular endothelial growth factor A/C.

From the [1]Division of Research, Central Texas Veterans Health Care System, [2]Scott & White Digestive Disease Research Center, [3]Department of Medicine, Division of Gastroenterology, [4]Division of Research and Education, and [5]Pathology, Scott & White Healthcare and Texas A&M Health Science Center, College of Medicine, Temple, TX; [6]Department of Biotechnological and Applied Clinical Sciences, State University of L'Aquila, L'Aquila, Italy; [7]Department of Anatomical, Histological, Forensic Medicine and Orthopedic Sciences, University "Sapienza," Rome, Italy; [8]Department of Gastroenterology, Yamagata University Faculty of Medicine, Yamagata, Japan; [9]Eleonora Lorillard Spencer Cenci Foundation, Rome, Italy, and [10]Department of Health Sciences, University of Rome "Foro Italico," Rome, Italy.

Received November 6, 2011; accepted October 3, 2012.

activation of protein kinase A (PKA), which results in the efflux of Cl^- through the cystic fibrosis transmembrane conductance regulator (CFTR),[4] and subsequent activation of the chloride bicarbonate anion exchanger 2 (Cl^-/HCO_3^- AE2)[5] stimulating bicarbonate secretion.[2]

Cholangiocytes are the target cells in human cholangiopathies[6] and animal models of cholestasis, such as bile duct ligation (BDL), a maneuver that induces proliferation of large, but not small, cholangiocytes.[2] Subsequent to BDL, biliary hyperplasia is coupled with enhanced functional expression of SR, CFTR, and Cl^-/HCO_3^- AE2 and increased secretory responses to secretin.[2,3,7] In the BDL model, small cholangiocytes proliferate *de novo* to compensate for the functional damage of large cholangiocytes (e.g., after CCl_4 administration).[8] The balance between biliary proliferation and damage is regulated by several autocrine factors, including vascular endothelial growth factor A/C (VEGF-A/C) and serotonin.[9,10]

Melatonin is an indole formed enzymatically from L-tryptophan by the enzymes, serotonin N-acetyltransferase (AANAT) and N-acetylserotonin O-methyltransferase (ASMT),[11] and is produced by the pineal gland as well as the small intestine and liver.[12,13] Melatonin ameliorates liver fibrosis and systemic oxidative stress (OS) in cholestatic rats.[14,15] Melatonin inhibits biliary hyperplasia and secretin-stimulated choleresis in BDL rats by interaction with melatonin type 1 (MT1) receptor by decreased PKA phosphorylation.[16] No information exists regarding the role of melatonin in the autocrine regulation of biliary growth. We proposed to evaluate the (1) expression of AANAT by cholangiocytes and (2) effects of *in vivo* and *in vitro* modulation of biliary AANAT and melatonin secretion on the proliferative and secretory responses of cholangiocytes by autocrine signaling.

Materials and Methods

Materials. All reagents were purchased from Sigma-Aldrich (St. Louis, MO), unless otherwise indicated. Antibodies used are detailed in the Supporting Materials. The RNeasy Mini Kit for RNA purification was purchased from Qiagen (Valencia, CA). Radioimmunoassay kits for measurement of cAMP levels were purchased from GE Healthcare (Arlington Heights, IL).

Animal Models. Male Fischer 344 rats (150-175 g; from Charles River Laboratories, Wilmington, MA) were housed at 22°C with 12-hour light/dark cycles and had free access to chow and drinking water. In addition to healthy (sham) rats, we used animals that, immediately after BDL, had free access to drinking water (vehicle) or melatonin (20 mg/L in drinking water)[16] for 1 week. This dose corresponds to a melatonin intake of approximately 2 mg/g body weight (BW)/day/rat.[16] This model of melatonin administration to rats has been previously validated and results in increased melatonin serum levels.[16] Animal experiments were performed in accordance with a protocol approved by the Scott & White and Texas A&M Health Science Center Institutional Animal Care and Use Committee (Temple, TX).

In separate experiments, healthy or BDL (immediately after surgery)[2] rats (n = 9 per group) were treated with Vivo-Morpholino sequences of AANAT (5′-GTTCCCCAGCTTTGGAAGTGGTCCC, to reduce hepatic expression of AANAT) or mismatched Morpholino (5′-GTTCCCGACCTTTGCAACTCGTCCC) (Gene Tools LCC, Philomath, OR) for 1 week by an implanted portal vein catheter (Supporting Materials). Serum, liver tissue, cholangiocytes, pineal gland, kidney, spleen, small intestine, stomach, and heart were collected. Because we aimed to selectively knock down AANAT expression in the liver, we used a lower dose (1.0 mg/kg BW/day) of Vivo-Morpholino than that previously described (3.0 mg/kg/day).[17] This approach minimizes the amount of Vivo-Morpholino that circulates outside of the liver after slow infusion into the portal vein.

Freshly Isolated and Immortalized Cholangiocytes. Pure small and large cholangiocytes were isolated by immunoaffinity separation.[4] *In vitro* studies were

This work was supported by the Dr. Nicholas C. Hightower Centennial Chair of Gastroenterology from Scott & White Hospital, the National Institutes of Health (NIH) (grant no.: DK062975; to G.A.), a Ministry of Education, Universities and Research (MIUR) grant (2003060137_004) to the Department of Gastroenterology, a grant award from Health and Labor Sciences Research Grants for the Research on Measures for Intractable Diseases (from the Ministry of Health, Labor, and Welfare of Japan) and from Grant-in-Aid for Scientific Research C (21590822) from the Japan Society for the Promotion of Science (JSPS; to T.U.) by University funds (to P.O.), University of Rome "Sapienza," and a MIUR grant (2009X84L84) and a funding for basic research grant (#RBAP10Z7FS) (to E.G.), and the NIH K01 grant award (DK078532) and NIH grant DK082435 (to S.D.M.).

Drs. Alpini, Glaser and Gaudio share the last authorship.

Address reprint requests to: Gianfranco Alpini, Ph.D., Scott & White Digestive Diseases Research Center, Central Texas Veterans Health Care System, Texas A & M Health Science Center College of Medicine, Olin E. Teague Medical Center, 1901 South 1st Street, Building 205, 1R60, Temple, TX 76504. E-mail: galpini@tamu.edu; fax: 743-0378 or 743-0555.

View this article online at wileyonlinelibrary.com.

DOI: 10.1002/hep.26105

Potential conflict of interest: Nothing to report.

Additional Supporting Information may be found in the online version of this article.

performed in immortalized large cholangiocytes (mouse cholangiocyte line [MCL]; from large bile ducts)[18] that are functionally similar to freshly isolated large cholangiocytes.[7,19] MCLs were cultured as previously described.[7]

Measurement of AANAT Expression and Melatonin Levels. We evaluated the (1) expression of AANAT in liver sections (4 μm thick) by immunohistochemistry (IHC)[20] and RNA (1 μg) and protein (10 μg) (by real-time polymerase chain reaction [PCR] and immunoblottings, respectively) from total liver, pooled, small, and/or large cholangiocytes (Supporting Materials)[16,21] and (2) effectiveness of AANAT Vivo-Morpholino in altering AANAT protein expression in liver sections by IHC[16] in total liver, cholangiocytes, pineal gland, and small intestine by immunoblottings[16] and melatonin levels by enzyme-linked immunosorbent assay (ELISA) kits in cholangiocytes from the selected groups of animals. IHC observations were taken in a coded fashion by a BX-51 light microscope (Olympus, Tokyo, Japan) with a Videocam (Spot Insight; Diagnostic Instruments, Inc., Sterling Heights, MI) and were analyzed with an image analysis system (IAS 2000; Delta Sistemi, Rome, Italy). Negative controls were included. A previously described method was used to quantify, in liver sections, the percent of bile ducts positive for AANAT.[18] When 0%-5% of bile ducts were positive, we assigned a negative score; a plus/minus score was assigned when 6%-10% of ducts were positive; and a plus score was assigned when 11%-30% of bile ducts were positive.[18] Melatonin levels in serum and medium of primary of cultures (after 6 hours of incubation at 37°C)[22] of cholangiocytes were determined by ELISA kits (Genway, San Diego, CA). We evaluated protein expression of cytokeratin-19 (CK-19) by immunoblottings[16] in cholangiocytes from healthy rats and BDL rats treated with vehicle or melatonin.

Evaluation of Histomorphology, Biliary Proliferation, Apoptosis, and Serum Chemistry. Connective tissue was quantified by Sirius red staining by analyzing liver sections with an image analysis system (IAS 2000; Delta Sistemi), and morphological changes in spleen, kidney, heart, stomach, and small intestine by hematoxylin and eosin (H&E) staining was measured. Biliary proliferation was determined by measurement of the percentage of proliferating cell nuclear antigen (PCNA)-positive cholangiocytes, with intrahepatic bile duct mass (IBDM) by IHC for CK-19.[20] Biliary apoptosis was evaluated by a semiquantitative terminal deoxynucleotidyl transferase dUTP nick-end labeling kit (Chemicon International, Inc., Temecula, CA).[20] Levels of serum glutamate pyruvate transaminases (SGPTs), serum glutamic oxaloacetic transaminase (SGOT), alkaline phosphatase (ALP), and total bilirubin (TBIL) were measured by a Dimension RxL Integrated Chemistry system (Dade Behring Inc., Deerfield IL) by the Chemistry Department at the Scott & White Digestive Diseases Research Center.

Effect of AANAT Knockdown on Expression of PCNA, SR, CFTR, and Cl^-/HCO_3^- AE2. We evaluated, by real-time PCR and/or immunoblottings, expression of PCNA, CK-19, SR, CFTR, and Cl^-/HCO_3^- AE2 in liver tissue and/or cholangiocytes from healthy and BDL rats treated with mismatch or AANAT Vivo-Morpholino. A delta delta of the threshold cycle analysis was obtained using normal total liver or healthy cholangiocytes, respectively, as control samples. Primers for rat PCNA, SR, CFTR, Cl^-/HCO_3^- AE2, and CK-19 (SABiosciences) were designed according to the following National Center for Biotechnology Information (NCBI) GenBank accession numbers: NM_022381 (PCNA); NM_031115 (SR); NM_017048 (Cl^-/HCO_3^- AE2); XM_001059206 (CFTR); and NM_199467 (CK-19). Messenger RNA (mRNA) data are expressed as ratio to CK-19 mRNA levels.

In Vitro ***Effect of Melatonin on Proliferation and Protein Expression of SR, CFTR, and Cl^-/HCO_3^- AE2 of Large Cholangiocytes.*** After trypsinization, MCLs were treated at 37°C for 24, 48, or 72 hours with 0.2% bovine serum albumin (BSA) or melatonin (10^{-11} M)[16] before evaluating cell proliferation by PCNA immunoblottings or MTS assays[16] and protein expression of SR, CFTR, Cl^-/HCO_3^- AE2 by fluorescence-activated cell sorting (FACS) analysis.[16]

Overexpression of AANAT in MCL and Measurement of Biliary Proliferative and Secretory Activities. MCLs were transfected using an AANAT complementary DNA clone vector from OriGene Technologies, Inc. (Rockville, MD), that confers resistance to geneticin for the selection of stable transfected cells. Transfected cells were selected by the addition of geneticin into the media, and the selection process was allowed to continue for 4-7 days.[23] Surviving cells (MCL-AANAT) were assessed for relative expression of AANAT, compared to control transfected cells (MCL-puro), by real-time PCR.[21] In the selected clone with the greatest degree of overexpression, we measured protein expression of AANAT (by FACS)[21,24] and melatonin secretion (after 6-hour incubation) by ELISA kits, compared to MCL-puro. In the two cell lines, we measured basal proliferative activity by (1) immunoblottings for PCNA (after 48-hour incubation)[21] and MTS assays (after 24-72 hours of incubation),[7] (2) determination of cell number by a hemocytometer chamber and the Cellometer Auto

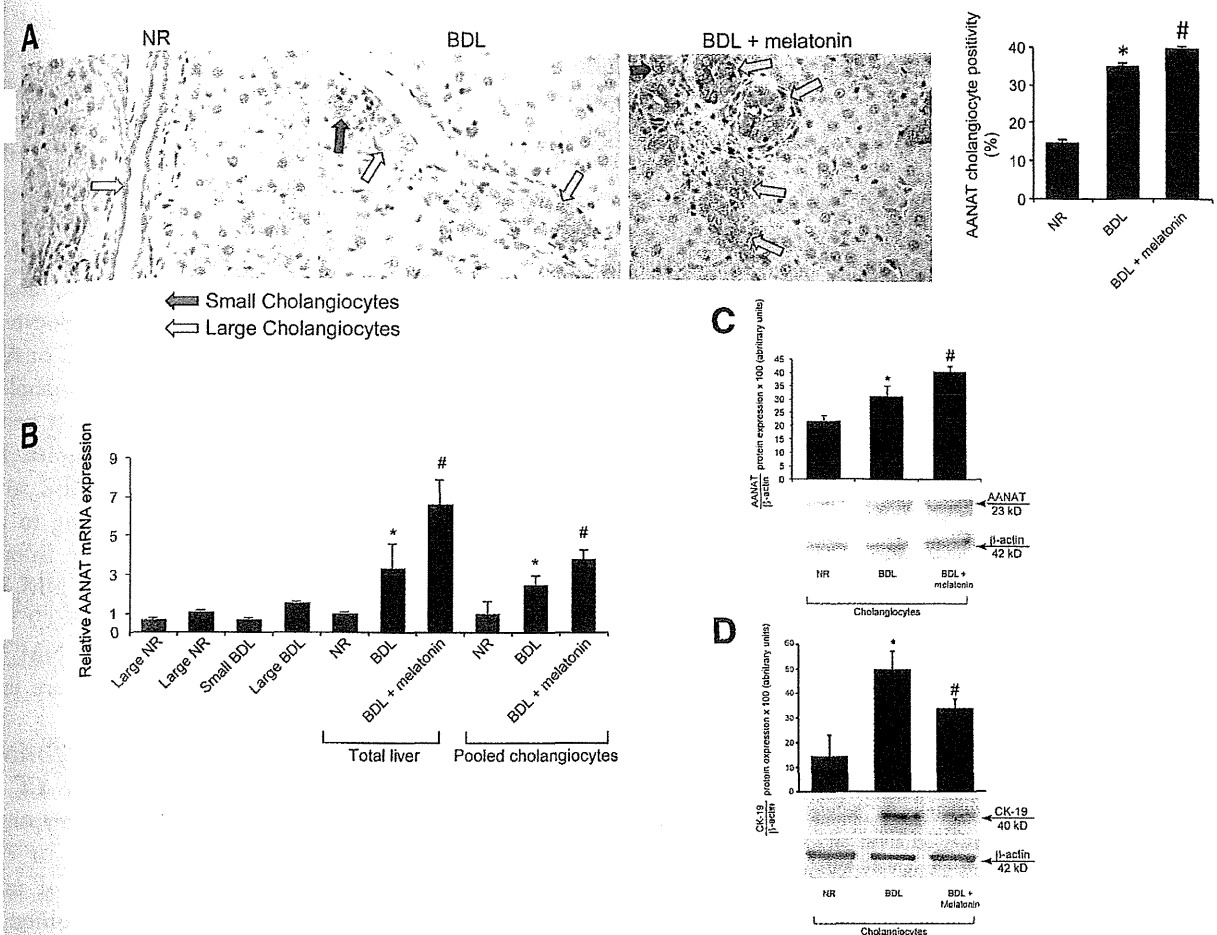

Fig. 1. (A) By IHC, AANAT was expressed by both small (red arrows) and large (yellow arrows) bile ducts from healthy and BDL rats. AANAT expression increased in bile ducts from BDL, compared to healthy, rats and in BDL rats treated with melatonin, compared to BDL rats. Values were obtained from IHC evaluation of 10 randomly selected fields of three slides obtained from 3 rats for each group. *$P < 0.05$ versus the corresponding value of healthy rats; #$P < 0.05$ versus the value of BDL rats. Original magnification, ×40. (B) By real-time PCR, AANAT was expressed by total liver and pooled, small, and large cholangiocytes from healthy and BDL rats. (B and C) By real-time PCR and/or immunoblottings, AANAT expression increased in total liver and pooled cholangiocytes from BDL rats, compared to healthy rats, and from BDL rats treated with melatonin, compared to BDL rats. (B) Data are mean ± SEM of six real-time reactions performed in cumulative preparations (resulting from the low cell yield from 1 rat) of cholangiocytes obtained from 6 rats. (C) Data are mean ± SEM of six immunoblottings performed in cumulative preparations of cholangiocytes obtained from 6 rats. *$P < 0.05$ versus the values of healthy rats; #$P < 0.05$ versus the value of BDL rats. (D) CK-19 expression increased in cholangiocytes from BDL, compared to healthy rats, and decreased in BDL rats treated with melatonin, compared to BDL rats. Data are mean ± SEM of six immunoblottings performed in cumulative preparations of cholangiocytes obtained from 6 rats. *$P < 0.05$ versus the corresponding value of healthy rats; #$P < 0.05$ versus the value of BDL rats.

(Nexcelom Bioscience, Lawrence, MA)[25] (after incubation for 24-72 hours), and (3) mRNA and protein expression for SR, CFTR, and Cl^-/HCO_3^- AE2 were evaluated by real-time PCR and FACs analysis, respectively.[21,24] Effects of secretin (10^{-7} M for 5 minutes) on cAMP levels[18,26] and Cl^- efflux, a functional index of CFTR activity,[4] were also evaluated. Primers for mouse SR, CFTR, Cl^-/HCO_3^- AE2, and glyceraldehyde-3-phosphate dehydrogenase (GAPDH) (SABiosciences) were designed according to the following NCBI GenBank accession numbers: NM_001012322 (SR); NM_021050 (CFTR); NM_009207 (Cl^-/HCO_3^- AE2); NM_009591 (AANAT); and NM_008084 (GAPDH). mRNA data are expressed as ratio to GAPDH mRNA levels.

Statistical Analysis. All data are expressed as mean ± standard error of the mean (SEM). Differences between groups were analyzed by Student unpaired *t* test when two groups were analyzed. Analysis of variance was utilized when more than two groups were analyzed, which was followed by an appropriate post-hoc test.

Results

Expression of AANAT. By IHC in liver sections, AANAT was expressed by small (red arrows) and large

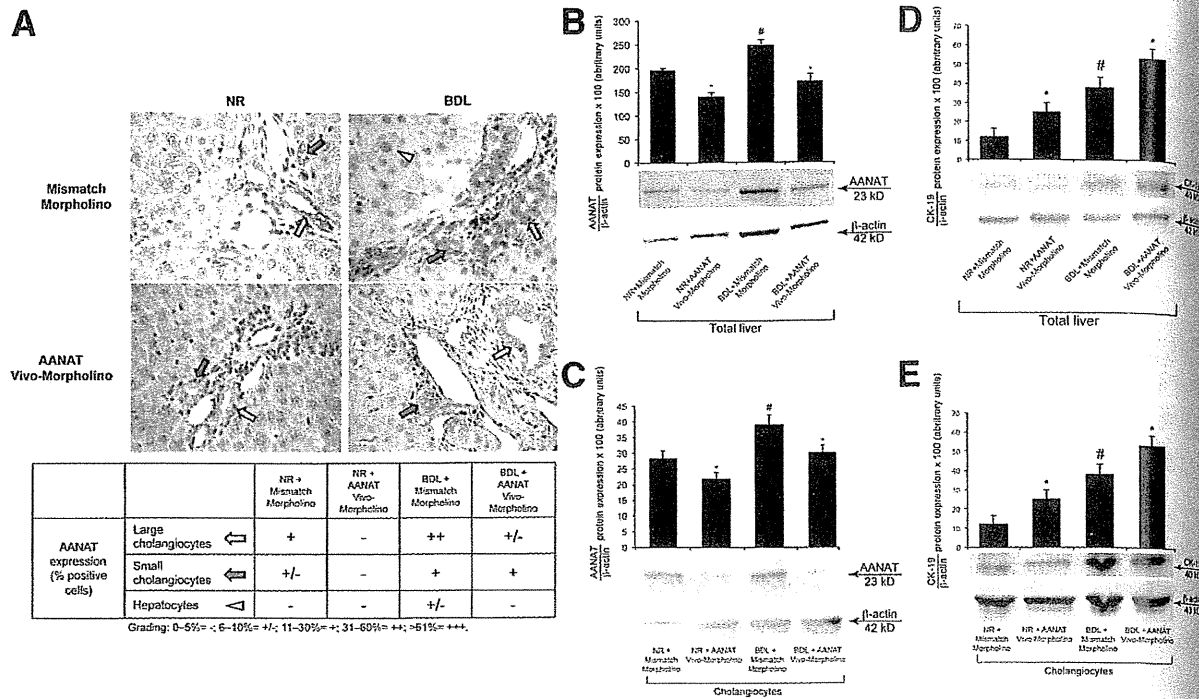

		NR + Mismatch Morpholino	NR + AANAT Vivo-Morpholino	BDL + Mismatch Morpholino	BDL + AANAT Vivo-Morpholino
AANAT expression (% positive cells)	Large cholangiocytes ⇦	+	-	++	+/-
	Small cholangiocytes ⇦	+/-	-	+	+
	Hepatocytes ◁	-	-	+/-	-

Grading: 0–5%= -; 6–10%= +/-; 11–30%= +; 31–60%= ++; >61%= +++.

Fig. 2. (A) AANAT was expressed by both small (red arrows) and large (yellow arrows) bile ducts from healthy and BDL rats. (A-C) AANAT protein expression decreased in bile ducts (in liver sections), total liver samples, and cholangiocytes from both healthy and BDL rats treated with AANAT Vivo-Morpholino, compared to controls. (A) Original magnification, ×40. Values were obtained from IHC evaluation of 10 randomly selected fields of three slides from 3 rats for each group. (B) Data are mean ± SEM of six immunoblottings performed in three different total liver samples obtained from 6 individual rats. (C) Data are mean ± SEM of six immunoblottings performed in cumulative preparations of cholangiocytes obtained from 6 rats. *$P < 0.05$ versus the corresponding value of rats treated with mismatch Morpholino. #$P < 0.05$ versus the corresponding value of healthy rats. (D and E) CK-19 protein expression increased in total liver and cholangiocytes from healthy and BDL rats treated with AANAT Vivo-Morpholino, compared to controls. (D) Data are mean ± SEM of six immunoblottings performed in three different total liver samples obtained from 6 individual rats. (E) Data are mean ± SEM of six immunoblottings performed in cumulative preparations of cholangiocytes obtained from 6 rats. *$P < 0.05$ versus the corresponding value of rats treated with mismatch Morpholino. #$P < 0.05$ versus the corresponding value of healthy rats.

(yellow arrows) bile ducts from healthy and BDL rats (Figs. 1A and 2A). AANAT expression increased in bile ducts from BDL, compared to healthy rats, and in BDL rats treated with melatonin, compared to BDL rats (Fig. 1A). Healthy hepatocytes were negative for AANAT, whereas scattered hepatocytes from BDL rats showed weak positivity for AANAT (Figs. 1A and 2A). By real-time PCR, AANAT was expressed by total liver as well as pooled, small, and large cholangiocytes from healthy and BDL rats (Fig. 1B). By both real-time PCR and/or immunoblottings, AANAT expression increased in total liver and pooled (which included small and large cholangiocytes) biliary epithelial cells from BDL, compared to healthy rats and from BDL rats treated with melatonin, compared to BDL rats (Fig. 1 B,C). CK-19 expression increased in cholangiocytes from BDL, compared to healthy rats and decreased in BDL rats treated with melatonin, compared to BDL rats (Fig. 1D).

AANAT protein expression decreased in bile ducts (in liver sections), total liver samples, and cholangiocytes from healthy and BDL rats treated with AANAT Vivo-Morpholino, compared to controls (Fig. 2A-C). AANAT protein expression increased in pineal gland and small intestine from healthy and BDL rats treated with AANAT Vivo-Morpholino, compared to controls (not shown). CK-19 protein expression increased in total liver and cholangiocytes from healthy and BDL rats treated with AANAT Vivo-Morpholino, compared to controls (Fig. 2 D,E).

Melatonin Levels in Serum and Cholangiocyte Supernatant. Melatonin levels were higher in supernatant of cholangiocytes from BDL, compared to healthy rats and increased in cholangiocyte samples from BDL rats treated with melatonin (Supporting Table 1). Consistent with previous studies,[16] melatonin serum levels were higher in BDL, compared to healthy, rats (Table 1). Melatonin serum levels increased in healthy and BDL rats treated with AANAT Vivo-Morpholino, compared to rats treated with mismatch Morpholino (Table 1). Although AANAT biliary expression decreased in rats treated with AANAT Vivo-Morpholino (Fig. 2 A-C), the increase in melatonin serum levels observed in these rats was likely a

Table 1. Evaluation of Melatonin Levels, Percentage of PCNA-Positive or Apoptotic Cholangiocytes, and Intrahepatic Bile Duct Mass and Serum Chemistry

Parameters	Normal Rats + Mismatch Morpholino	Normal Rats + AANAT Vivo-Morpholino	BDL Rats + Mismatch Morpholino	BDL Rats + AANAT Vivo-Morpholino
Serum melatonin levels (pg/mL)	70.9 ± 1.1 (n = 5)	77.6 ± 2.9* (n = 5)	97.5 ± 2.8† (n = 5)	174.1 ± 11.7‡ (n = 5)
Cholangiocyte melatonin levels (pg/ml)	43.9 ± 4 (n = 4)	26.9 ± 4.01* (n = 4)	61.5 ± 3.5† (n = 4)	39.5 ± 1.44‡ (n = 4)
% PCNA-positive cholangiocytes	6.80 ± 2.13	10.24 ± 1.17*	58.07 ± 7.25†	68.10 ± 4.94‡
IBDM (%)	0.22 ± 0.1	0.41 ± 0.08*	2.32 ± 0.41†	4.75 ± 1.60‡
% apoptotic cholangiocytes	Not detected	Not detected	4.12 ± 2.30	Not detected
SGPT (Units/L)	62.6 ± 7.7 (n = 9)	70 ± 1.25 (n = 9)	194.4 ± 17 (n = 9)	121.2 ± 19§ (n = 9)
SGOT (Units/L)	129 ± 7 (n = 9)	148 ± 5.1 (n = 9)	614.5 ± 68.3 (n = 9)	312 ± 52§ (n = 9)
ALP (Units/L)	203 ± 6.6 (n = 9)	202.8 ± 8 (n = 9)	395 ± 9.8 (n = 9)	343.2 ± 18.7§ (n = 9)
TBIL (mg/L)	<0.1 (n = 9)	<0.1 (n = 9)	8.7 ± 0.5 (n = 9)	7.5 ± 0.6§ (n = 9)

Data are mean ± SEM. IBDM represents area occupied by CK-19-positive bile duct/total area × 100.
*$P < 0.05$ versus the corresponding value of normal rats treated with mismatch Morpholino.
†$P < 0.05$ versus the corresponding value of normal rats treated with mismatch Morpholino AANAT Vivo-Morpholino.
‡$P < 0.05$ versus all other groups.
§$P < 0.05$ versus the corresponding value of BDL rats treated with mismatch Morpholino.

result of enhanced expression of AANAT (and subsequent increased melatonin secretion) in the pineal gland and small intestine, which also express AANAT.[13,27] Melatonin levels decreased in supernatant of cholangiocytes from healthy and BDL rats treated with AANAT Vivo-Morpholino, compared to controls (Table 1).

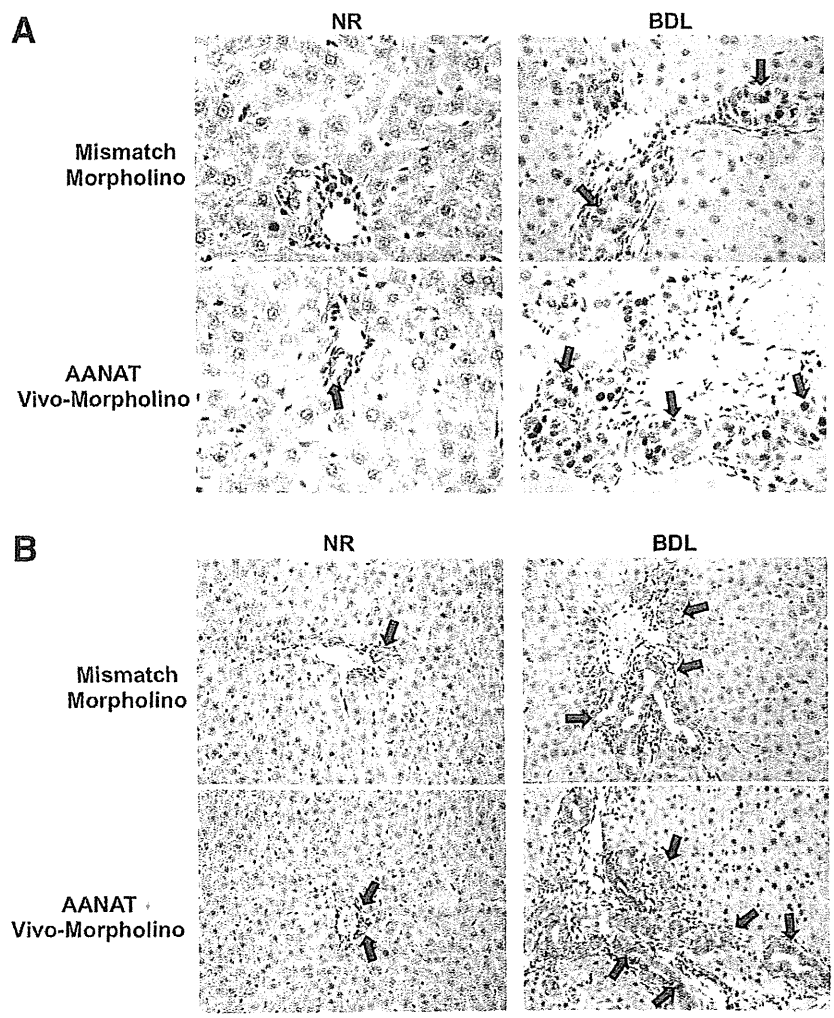

Fig. 3. Evaluation of the percentage of (A) PCNA-positive cholangiocytes and (B) IBDM in liver sections from the selected groups of animals. In rats treated with AANAT Vivo-Morpholino, there was an enhanced percentage of PCNA-positive cholangiocytes and IBDM, compared to controls (for semiquantitative analysis, see Table 1). (A) Percentage of PCNA-positive cholangiocytes was assessed in 10 randomly selected fields of three slides obtained from 3 different animals for each group. Positive cells were counted in six nonoverlapping fields for each slide. Original magnification, ×40. (B) Percentage surface occupied by CK-19-positive cholangiocytes (IBDM) was assessed in 10 randomly selected fields of three slides. *$P < 0.05$ versus the corresponding value of healthy rats treated with mismatch Morpholino. Original magnification, ×20.

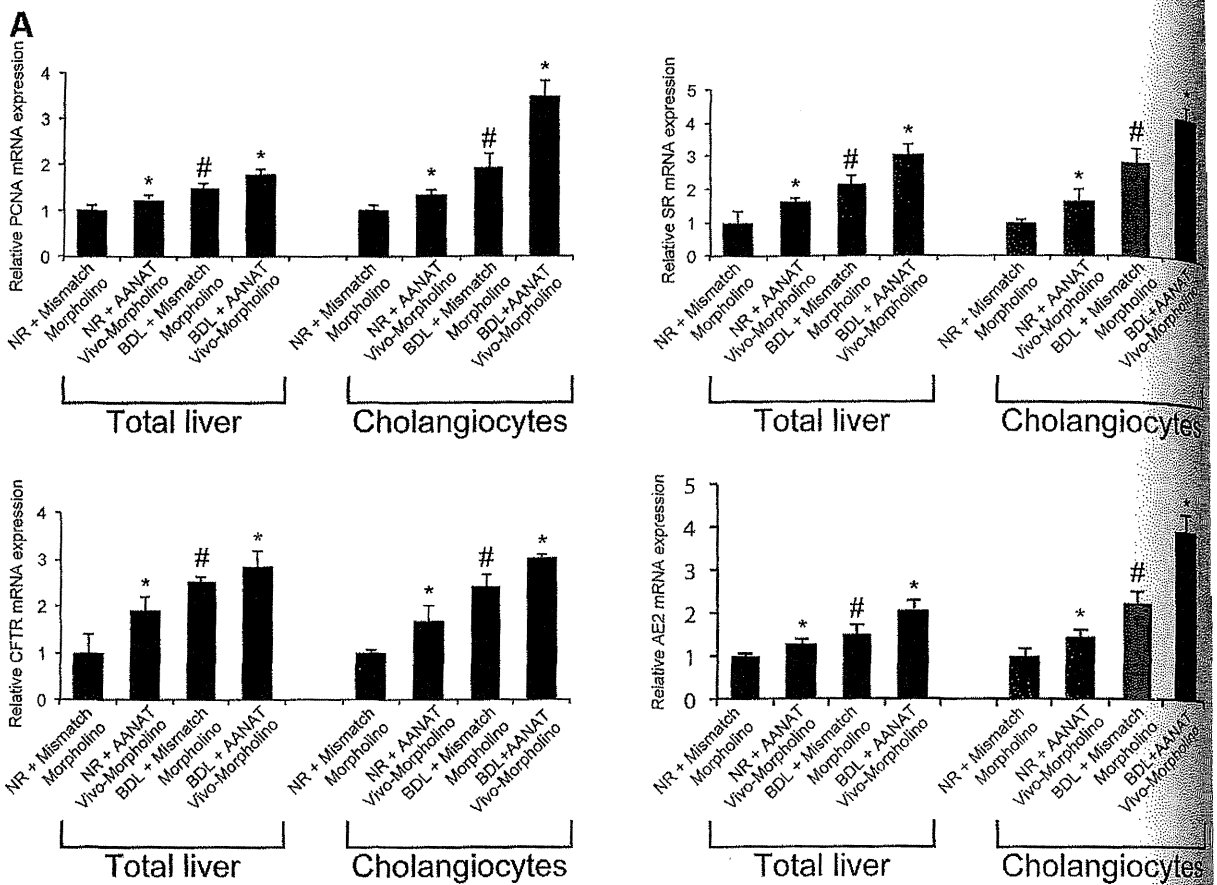

Fig. 4. (A) Effect of AANAT knockdown on mRNA expression of PCNA, SR, CFTR, and Cl^-/HCO_3^- AE2 in lysate from total liver samples and isolated cholangiocytes. Increased mRNA expression of PCNA, SR, CFTR, and Cl^-/HCO_3^- AE2 was observed in total liver and cholangiocytes from healthy and BDL rats treated with AANAT Vivo-Morpholino, compared to controls. Data are mean ± SEM of six real-time reactions performed in cumulative preparations (resulting from the low cell yield from 1 rat) of cholangiocytes obtained from 6 rats. *$P < 0.05$ versus the corresponding value of healthy and BDL rats treated with mismatch Morpholino. #$P < 0.05$ versus the corresponding value of healthy rats treated with mismatch Morpholino. (B) Effect of AANAT knockdown on protein expression of PCNA, SR, CFTR, and Cl^-/HCO_3^- AE2 in lysate from isolated cholangiocytes. Increased expression of PCNA, SR, CFTR, and Cl^-/HCO_3^- AE2 was observed in cholangiocytes from normal and BDL rats treated with AANAT Vivo-Morpholino, compared to controls. Data are mean ± SEM of six immunoblottings performed in cumulative preparations of cholangiocytes obtained from 6 rats. *$P < 0.05$ versus the corresponding value of healthy and BDL rats treated with mismatch Morpholino. #$P < 0.05$ versus the corresponding value of healthy rats treated with mismatch Morpholino.

Evaluation of Histomorphology, Biliary Proliferation, Apoptosis, and Serum Chemistry. In liver sections from healthy and BDL rats treated with AANAT Vivo-Morpholino, there was increased percentage of PCNA-positive cholangiocytes and IBDM, compared to controls (Fig. 3A,B; Table 1). No changes in biliary apoptosis (Table 1) were observed between healthy and BDL rats treated with AANAT Vivo-Morpholino, compared to healthy rats treated with mismatch Morpholino. No difference in lobular damage or necrosis was observed for healthy versus BDL rats treated with AANAT Vivo-Morpholino, compared to controls (not shown). A similar degree of portal inflammation was observed between healthy and BDL rats treated with AANAT Vivo-Morpholino, compared to controls (not shown). Serum levels of transaminases, ALP, and TBIL decreased in BDL rats treated with Vivo-Morpholino, compared to rats treated with mismatch-Morpholino (Table 1). In BDL Mismatch-treated rats, we found that connective tissue represents approximately 1.5% of the liver whereas in BDL rats treated with AANAT Vivo-Morpholino, collagen tissues represented approximately 3% of liver mass (not shown). None of the organs analyzed by H&E staining showed structural damage, necrosis, or inflammation (not shown).

Effect of AANAT Knockdown on Expression of PCNA, SR, CFTR, and Cl^-/HCO_3^- AE2. There was increased expression of mRNA (Fig. 4A) and protein (Fig. 4B) of PCNA, SR, CFTR, and Cl^-/HCO_3^- AE2 in cholangiocytes from rats treated with AANAT Vivo-Morpholino, compared to controls (Fig. 4B).

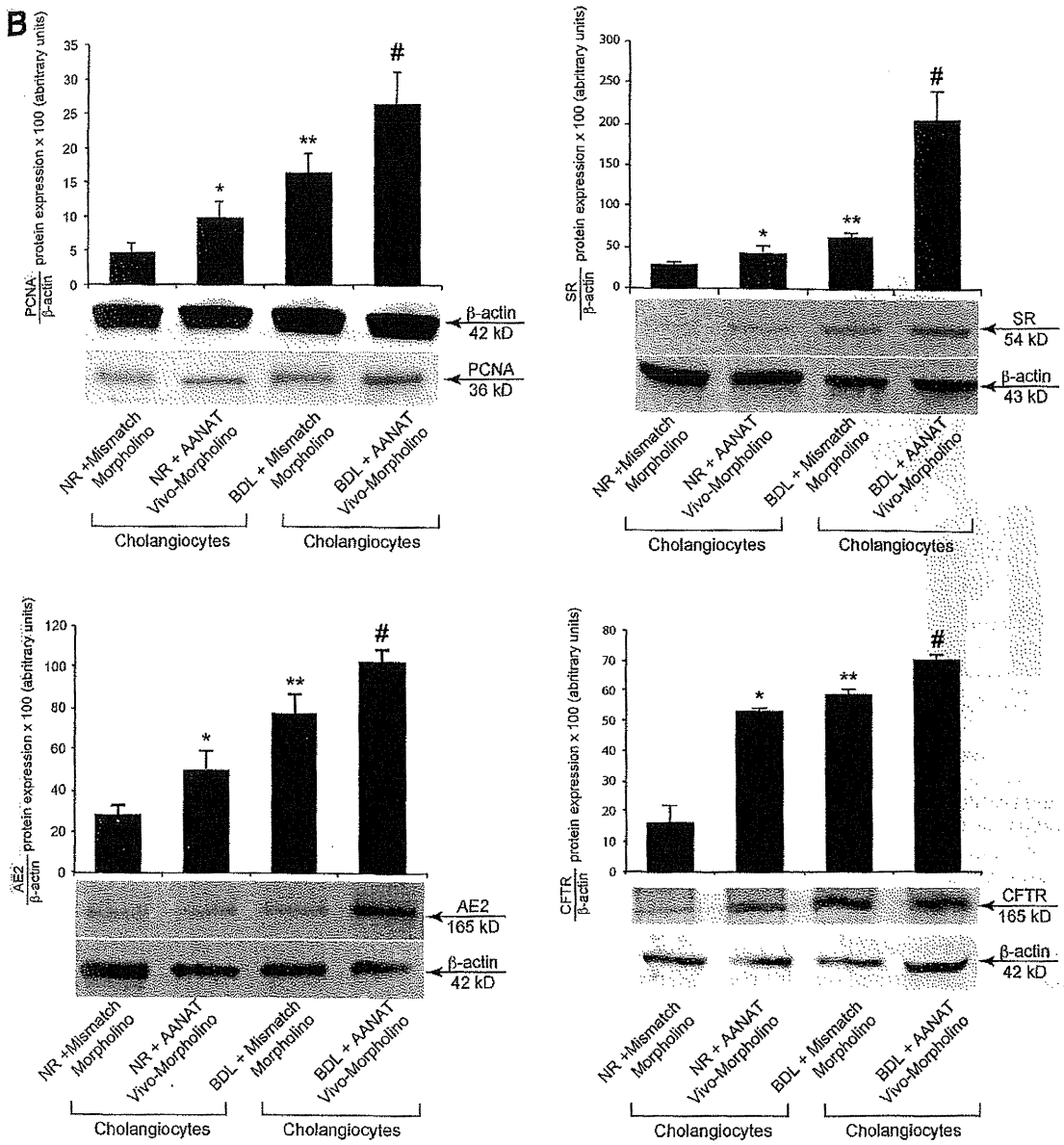

Fig. 4.

In Vitro ***Effect of Melatonin on the Proliferation and Protein Expression of SR, CFTR, and Cl^-/HCO_3^- AE2 of Large Cholangiocytes.*** *In vitro*, melatonin inhibited biliary proliferation (by MTS assays and PCNA immunoblottings; Supporting Fig. 1) and protein expression (by FACS analysis) of SR, CFTR, and Cl^-/HCO_3^- AE2, compared to large cholangiocytes treated with 0.2% BSA (Supporting Fig. 1).

Effect of Overexpression of AANAT in MCL on Expression of PCNA, SR, CFTR, and Cl^-/HCO_3^- AE2. Enhanced mRNA and protein expression for AANAT and increased melatonin secretion were observed in AANAT-transfected cholangiocytes, compared to controls (Supporting Fig. 2A-C). In cholangiocytes overexpressing AANAT, there was (1) decreased biliary proliferation shown by PCNA immunoblottings and MTS assays (Fig. 5A,B) and a reduced number of cholangiocytes (Supporting Table 2) and (2) reduced mRNA (Fig. 5C-E) and protein (by FACS analysis; Fig. 5F) expression for SR, CFTR, and Cl^-/HCO_3^- AE2, compared to control cholangiocytes. Secretin did not increase cAMP levels (a functional index of SR expression)[4,28] and Cl^- efflux (a functional parameter of CFTR activity)[4] at 360 seconds after treatment with secretin in stably AANAT-overexpressing cholangiocytes (Supporting Fig. 3A,B).

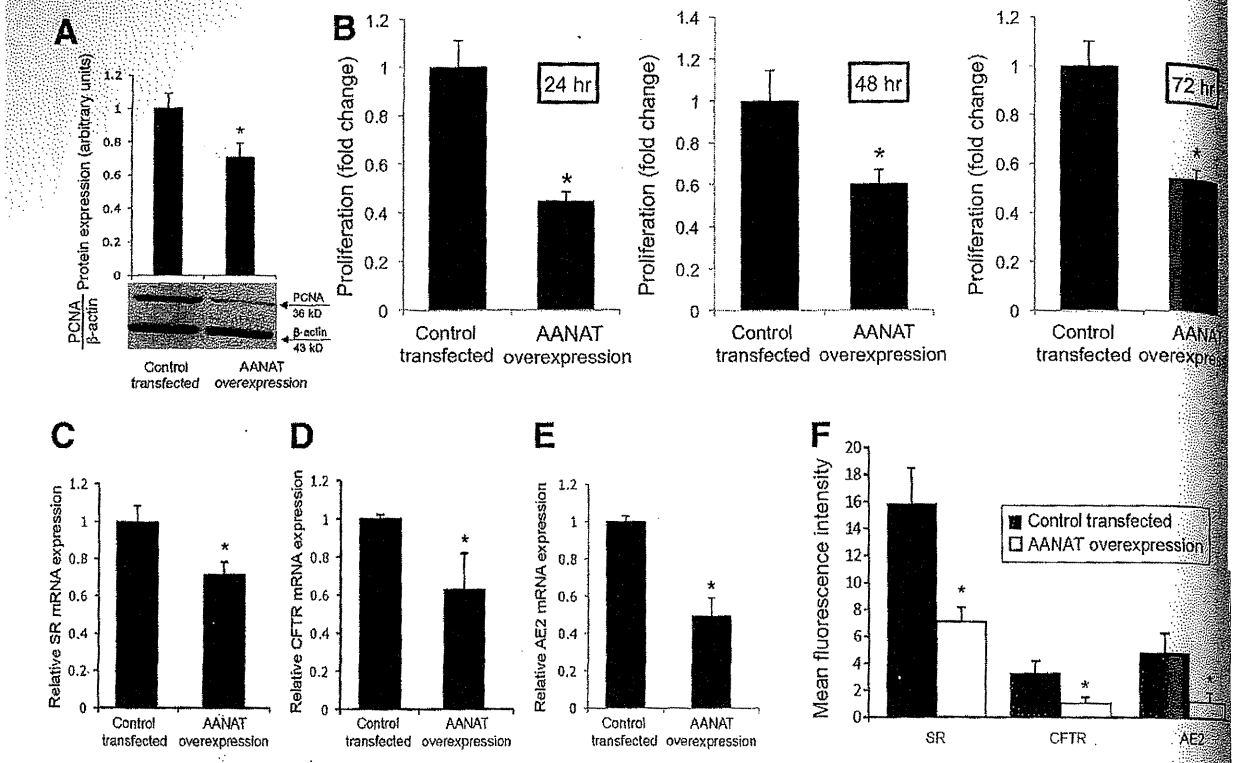

Fig. 5. In cholangiocytes overexpressing AANAT, (A and B) decreased biliary proliferation was observed, as shown by PCNA immunob and MTS assays as well as reduced (C-E) mRNA and (F) protein expression (by FACS analysis) for SR, CFTR, and Cl^-/HCO_3^- AE2, compar control cholangiocytes. (A and B) Data are mean ± SEM of six immunoblottings and MTS reactions performed in six different samples ob from cholangiocyte lines. (C-E) Data are mean ± SEM of six real-time PCR reactions performed in six different samples obtained from chol cyte lines. (F) Data are mean ± SEM of four different FACS analyses performed in four different samples obtained from cholangiocyte lines < 0.05 versus the corresponding value of cholangiocytes transfected with control vector.

Secretin stimulated cAMP and Cl^- efflux in large cholangiocytes transfected with the control vector (Supporting Fig. 3A,B).

Discussion

The data demonstrate that (1) AANAT is expressed by both small and large cholangiocytes and (2) local modulation of AANAT expression alters large cholangiocyte growth and secretin-stimulated ductal secretion. We demonstrated that (1) AANAT is expressed by bile ducts, and AANAT expression is up-regulated after BDL and by the administration of melatonin to BDL rats; weak immunoreactivity is present in BDL hepatocytes and (2) AANAT expression is decreased in liver samples and cholangiocytes from both healthy and BDL rats treated with AANAT Vivo-Morpholino, compared to controls. Concomitant with reduced AANAT biliary expression, there was increased proliferation and IBDM in liver sections and enhanced expression of PCNA, SR, CFTR, and Cl^-/HCO_3^- AE2 in cholangiocytes from healthy and BDL rats treated with AANAT Vivo-Morpholino, compared to controls. Serum levels of transaminases, ALP, and bilirubin decreased in AANAT Vivo-Morpholi treated BDL rats, confirming the improvement of lestasis after modulation of AANAT, likely the of increased melatonin serum levels. In support of findings, we have previously shown that serum l of transaminases and bilirubin increased in BDL r pared to healthy rats and decreased after admini tion of melatonin.[16] *In vitro* overexpression of AA in large cholangiocytes decreased (1) biliary proli tion, mitosis, and expression of SR, CFTR, and HCO_3^- AE2 and (2) secretin-stimulated cAMP l and Cl^- efflux, a functional index of C activity.[4,29]

Growing information is evident regarding auto regulation of cholangiocyte growth and damag autocrine factors.[9,10] Serotonin regulates hyper neoplastic biliary growth, both *in vivo* and *vitro*.[30,31] Blocking VEGF secretion decreases cho giocyte proliferation, revealing an autocrine wherein cholangiocytes secrete VEGF interacting VEGF receptors 2 and 3 to increase biliary proli tion.[10] In cholangiocytes from polycystic liver-di

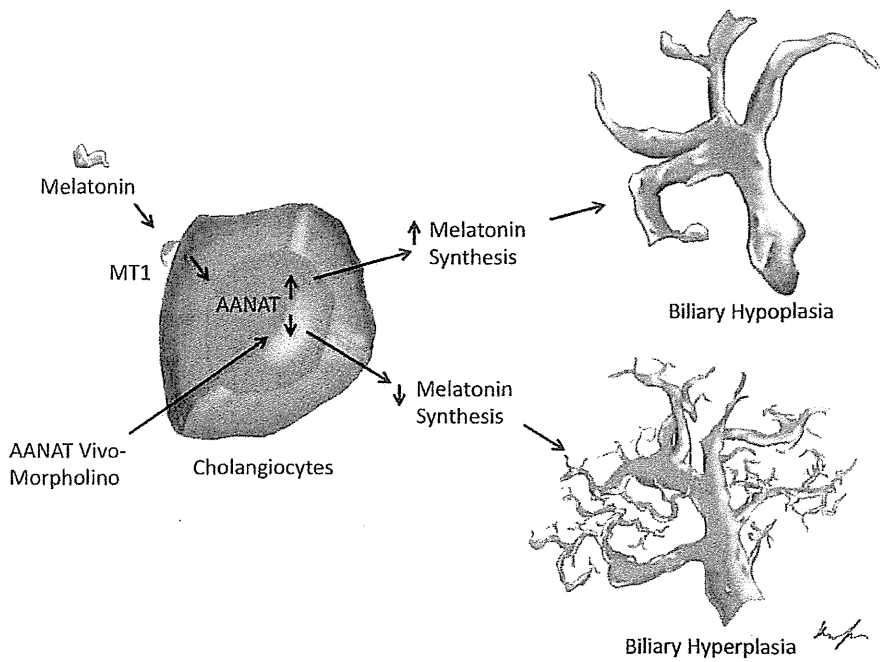

Fig. 6. Working model of changes induced by local modulation of AANAT in large biliary proliferation. Top: exogenous melatonin, by interaction with MT1 receptor, inhibits large cholangiocyte proliferation (hypoplasia) by increasing biliary AANAT expression and then melatonin secretion. Bottom: down-regulation of biliary AANAT levels by Vivo-Morpholino stimulates the proliferation of large cholangiocytes by reduction of biliary AANAT expression and melatonin secretion, which induces subsequent activation of biliary proliferation (hyperplasia).

samples, VEGF expression is up-regulated and VEGF supports cholangiocyte proliferation by autocrine mechanisms.[32] Although melatonin synthesis is dysregulated in cholangiocarcinoma,[33] no data exist regarding the autocrine role of melatonin (secreted by cholangiocytes) in the regulation of biliary hyperplasia.

Morpholinos are free of off-target effects because they are not degraded in biological systems and do not generate degradation products toxic to cells.[34] Phosphorodiamidate Morpholino oligomers have been used to evaluate the role of β-catenin in cell proliferation and apoptosis and early biliary lineage commitment of bipotential stem cells in the developing liver.[35] In zebrafish, Morpholino antisense oligonucleotide-mediated knockdown of planar-cell polarity genes led to developmental biliary abnormalities as well as localization defects of the liver.[36]

We first measured the expression of AANAT in liver sections, total liver and cholangiocytes, and melatonin serum levels in our models. The reason why we measured AANAT expression in healthy and BDL rats, and BDL rats treated with melatonin, was to demonstrate a link between AANAT expression and cholangiocyte proliferation in well-established models of biliary hyperplasia (BDL)[2,16] and reduced biliary hyperplasia (BDL + melatonin).[16] The increase of AANAT biliary expression and melatonin secretion after BDL are likely the result of a compensatory mechanism and correlates with increased melatonin serum levels observed in cholestatic rats,[16] an increase that may result from enhanced secretion of melatonin not only from cholangiocytes, but also from the small intestine and pineal gland.[12,13] The increase in AANAT expression by the pineal gland may result from a compensatory mechanism to ameliorate cholestatic-induced OS.[37] The enhanced biliary expression of AANAT in melatonin-treated BDL rats is supported by studies in rats and humans.[16,38] The reduction of biliary AANAT expression and melatonin secretion in cholangiocytes (after AANAT Vivo-Morpholino administration) supports the validity of the model and the hypothesis that the AANAT expression⇒melatonin secretion axis may be an important autocrine loop regulating locally biliary proliferation. The increase in melatonin serum levels observed in rats treated with AANAT Vivo-Morpholino was likely a result of the higher expression of AANAT (and likely melatonin secretion) by other sites, such as pineal glands and intestine, to compensate for the loss of biliary AANAT expression. The current findings do not exclude that other paracrine pathways (e.g., melatonin released from the pineal gland and/or hyperplastic hepatocytes) are important for the regulation of biliary function. In the healthy state, cholangiocytes represent approximately 2%-4% of the total liver cell population; however, after BDL cholangiocytes proliferate, and 1 week after BDL, biliary mass represents approximately 25%-30% of the total liver mass.[2] Hepatocytes may have a role (scattered) in the modulation of biliary proliferation, but in light of our findings (the reduced AANAT biliary expression by Morpholino enhances IBDM *in vivo*, and overexpression of AANAT *in vitro* decreases biliary

proliferation), we propose that AANAT has a role in the modulation of biliary proliferation, which probably is not the main, or the only one, acting factor on cholangiocytes. Studies aimed to evaluate the effects of changes in the central synthesis of melatonin (e.g., after pinealectomy and exposure to dark to stimulate melatonin release from the pineal gland) in the regulation of biliary functions are ongoing.

Having demonstrated that AANAT is expressed by cholangiocytes and that AANAT expression is up-regulated by BDL and melatonin administration, we proposed to demonstrate that reduction of biliary AANAT expression (by Vivo-Morpholino) increases cholangiocyte proliferation and IBDM as well as the expression of SR, CFTR, and Cl^-/HCO_3^- AE2 in cholangiocytes. After BDL, the increase of biliary proliferation and IBDM is followed by the extension of the peribiliary plexus and the increase of surrounding connective tissue, which is organized around bile ducts and vessels.[10] In our model, we only observed a slight difference in collagen tissue content in BDL rats treated with mismatch Morpholino versus BDL rats treated with AANAT Vivo-Morpholino. This low increase of connective tissue cannot determine a clear hepatic fibrosis in our model of short time of BDL. Further studies are needed to evaluate the long-term effects of BDL on the modulation of melatonin synthesis on liver fibrosis. Also, the novel concept that AANAT regulates SR⇒CFTR⇒Cl^-/HCO_3^- AE2 expression is supported by our previous study[16] showing that *in vivo* administration of melatonin to BDL rats decreases secretin-induced choleresis.

To determine that the effects of down-regulation of AANAT on biliary growth depend on direct effects on bile ducts, cholangiocytes were treated *in vitro* with melatonin that decreased the biliary proliferation and expression of SR, CFTR, and Cl^-/HCO_3^- AE2. We overexpressed AANAT in cholangiocytes and demonstrated a decrease in biliary proliferation and secretin-stimulated cAMP levels and Cl^- efflux. *In vitro*, overexpression of AANAT in cholangiocytes leading to decreased biliary proliferation and secretin receptor-dependent ductal secretion (in the absence of intestinal secretin supply) was likely the result of the fact that cholangiocytes express SR and express the message for secretin and secrete secretin,[7,39,40] which (similar to what is observed *in* vivo) is an important autocrine factor sustaining biliary proliferation. We propose that the modulation of biliary melatonin secretion (by chronic administration of melatonin or changes in AANAT expression; Fig. 6) may be a valuable therapeutic approach for regulating the balance between biliary growth/apoptosis. In support of this view, we have shown that in the first stage of primary biliary cirrhosis, there is an increase of cholangiocyte proliferation that resulted in a positive balance between growth and apoptosis.[41] By contrast, the end stage is characterized by the collapse of the proliferative capacity of cholangiocytes, resulting in the reduction (high apoptosis rate) of the number of bile ducts (vanishing bile duct syndrome).[41] Because, in our model, we have shown that the modulation of melatonin synthesis is involved in the balance between biliary growth and apoptosis, modulation of melatonin synthesis can be proposed as a possible strategy for the management of cholangiopathologies.

References

1. Kanno N, LeSage G, Glaser S, Alpini G. Regulation of cholangiocyte bicarbonate secretion. Am J Physiol Gastrointest Liver Physiol 2001; 281:G612-G625.
2. Alpini G, Lenzi R, Sarkozi L, Tavoloni N. Biliary physiology in rats with bile ductular cell hyperplasia. Evidence for a secretory function of proliferated bile ductules. J Clin Invest 1988;81:569-578.
3. Alpini G, Ulrich CD, 2nd, Phillips JO, Pham LD, Miller LJ, LaRusso NF. Upregulation of secretin receptor gene expression in rat cholangiocytes after bile duct ligation. Am J Physiol Gastrointest Liver Physiol 1994;266:G922-G928.
4. Alpini G, Ulrich C, Roberts S, Phillips JO, Ueno Y, Podila PV, et al. Molecular and functional heterogeneity of cholangiocytes from rat liver after bile duct ligation. Am J Physiol Gastrointest Liver Physiol 1997; 272:G289-G297.
5. Alvaro D, Cho WK, Mennone A, Boyer JL. Effect of secretion on intracellular pH regulation in isolated rat bile duct epithelial cells. J Clin Invest 1993;92:1314-1325.
6. Alpini G, Prall RT, LaRusso NF. The pathobiology of biliary epithelia. In: Arias IM, Boyer JL, Chisari FV, Fausto N, Jakoby W, Schachter D, et al., eds. The Liver: Biology and Pathobiology, 4th edition. Philadelphia, PA: Lippincott Williams & Wilkins; 2001:421-435.
7. Glaser S, Lam IP, Franchitto A, Gaudio E, Onori P, Chow BK, et al. Knockout of secretin receptor reduces large cholangiocyte hyperplasia in mice with extrahepatic cholestasis induced by bile duct ligation. Hepatology 2010;52:204-214.
8. LeSage G, Glaser S, Marucci L, Benedetti A, Phinizy JL, Rodgers R, et al. Acute carbon tetrachloride feeding induces damage of large, but not small cholangiocytes from BDL rat liver. Am J Physiol Gastrointest Liver Physiol 1999;276:G1289-G1301.
9. Alvaro D, Mancino MG, Glaser S, Gaudio E, Marzioni M, Francis H, Alpini G. Proliferating cholangiocytes: a neuroendocrine compartment in the diseased liver. Gastroenterology 2007;132:415-431.
10. Gaudio E, Barbaro B, Alvaro D, Glaser S, Francis H, Ueno Y, et al. Vascular endothelial growth factor stimulates rat cholangiocyte proliferation via an autocrine mechanism. Gastroenterology 2006;130: 1270-1282.
11. Iuvone PM, Tosini G, Pozdeyev N, Haque R, Klein DC, Chaurasia SS. Circadian clocks, clock networks, arylalkylamine N-acetyltransferase, and melatonin in the retina. Prog Retin Eye Res 2005;24:433-456.
12. Reiter RJ. Pineal melatonin: cell biology of its synthesis and of its physiological interactions. Endocr Rev 1991;12:151-180.
13. Bubenik GA. Gastrointestinal melatonin: localization, function, and clinical relevance. Dig Dis Sci 2002;47:2336-2348.
14. Esrefoglu M, Gul M, Emre MH, Polat A, Selimoglu MA. Protective effect of low dose of melatonin against cholestatic oxidative stress after common bile duct ligation in rats. World J Gastroenterol 2005;11:1951-1956.

15. Tahan G, Akin H, Aydogan F, Ramadan SS, Yapicier O, Tarcin O, et al. Melatonin ameliorates liver fibrosis induced by bile-duct ligation in rats. Can J Surg 2010;53:313-318.
16. Renzi A, Glaser S, DeMorrow S, Mancinelli R, Meng F, Franchitto A, et al. Melatonin inhibits cholangiocyte hyperplasia in cholestatic rats by interaction with MT1 but not MT2 melatonin receptors. Am J Physiol Gastrointest Liver Physiol 2011;301:G634-G643.
17. Arora V, Knapp DC, Reddy MT, Weller DD, Iversen PL. Bioavailability and efficacy of antisense morpholino oligomers targeted to c-myc and cytochrome P-450 3A2 following oral administration in rats. J Pharm Sci 2002;91:1009-1018.
18. Glaser S, Gaudio E, Rao A, Pierce LM, Onori P, Franchitto A, et al. Morphological and functional heterogeneity of the mouse intrahepatic biliary epithelium. Lab Invest 2009;89:456-469.
19. Ueno Y, Alpini G, Yahagi K, Kanno N, Moritoki Y, Fukushima K, et al. Evaluation of differential gene expression by microarray analysis in small and large cholangiocytes isolated from normal mice. Liver Int 2003;23:449-459.
20. Mancinelli R, Franchitto A, Gaudio E, Onori P, Glaser S, Francis H, et al. After damage of large bile ducts by gamma-aminobutyric acid, small ducts replenish the biliary tree by amplification of calcium-dependent signaling and de novo acquisition of large cholangiocyte phenotypes. Am J Pathol 2010;176:1790-1800.
21. Francis H, Glaser S, DeMorrow S, Gaudio E, Ueno Y, Venter J, et al. Small mouse cholangiocytes proliferate in response to H1 histamine receptor stimulation by activation of the IP_3/CaMK I/CREB pathway. Am J Physiol Cell Physiol 2008;295:C499-C513.
22. Glaser S, DeMorrow S, Francis H, Ueno Y, Gaudio E, Vaculin S, et al. Progesterone stimulates the proliferation of female and male cholangiocytes via autocrine/paracrine mechanisms. Am J Physiol Gastrointest Liver Physiol 2008;295:G124-G136.
23. Mancinelli R, Onori P, Gaudio E, DeMorrow S, Franchitto A, Francis H, et al. Follicle-stimulating hormone increases cholangiocyte proliferation by an autocrine mechanism via cAMP-dependent phosphorylation of ERK1/2 and Elk-1. Am J Physiol Gastrointest Liver Physiol 2009; 297:G11-G26.
24. Onori P, Wise C, Gaudio E, Franchitto A, Francis H, Carpino G, et al. Secretin inhibits cholangiocarcinoma growth via dysregulation of the cAMP-dependent signaling mechanisms of secretin receptor. Int J Cancer 2010;127:43-54.
25. Yang L, Wu X, Wang Y, Zhang K, Wu J, Yuan YC, et al. FZD7 has a critical role in cell proliferation in triple negative breast cancer. Oncogene 2011;30:4437-4446.
26. Francis H, LeSage G, DeMorrow S, Alvaro D, Ueno Y, Venter J, et al. The alpha2-adrenergic receptor agonist UK 14,304 inhibits secretin-stimulated ductal secretion by downregulation of the cAMP system in bile duct-ligated rats. Am J Physiol Cell Physiol 2007;293: C1252-C1262.
27. Humphries A, Wells T, Baler R, Klein DC, Carter DA. Rodent Aanat: intronic E-box sequences control tissue specificity but not rhythmic expression in the pineal gland. Mol Cell Endocrinol 2007; 270:43-49.
28. Alpini G, Glaser SS, Ueno Y, Pham L, Podila PV, Caligiuri A, et al. Heterogeneity of the proliferative capacity of rat cholangiocytes after bile duct ligation. Am J Physiol Gastrointest Liver Physiol 1998;274: G767-G775.
29. Basavappa S, Middleton J, Mangel AW, McGill JM, Cohn JA, Fitz JG. Cl^- and K^+ transport in human biliary cell lines. Gastroenterology 1993;104:1796-1805.
30. Marzioni M, Glaser S, Francis H, Marucci L, Benedetti A, Alvaro D, et al. Autocrine/paracrine regulation of the growth of the biliary tree by the neuroendocrine hormone serotonin. Gastroenterology 2005;128:121-137.
31. Alpini G, Invernizzi P, Gaudio E, Venter J, Kopriva S, Bernuzzi F, et al. Serotonin metabolism is dysregulated in cholangiocarcinoma, which has implications for tumor growth. Cancer Res 2008;68:9184-9193.
32. Fabris L, Cadamuro M, Fiorotto R, Roskams T, Spirli C, Melero S, et al. Effects of angiogenic factor overexpression by human and rodent cholangiocytes in polycystic liver diseases. HEPATOLOGY 2006;43: 1001-1012.
33. Han Y, Demorrow S, Invernizzi P, Jing Q, Glaser S, Renzi A, et al. Melatonin exerts by an autocrine loop antiproliferative effects in cholangiocarcinoma: its synthesis is reduced favoring cholangiocarcinoma growth. Am J Physiol Gastrointest Liver Physiol 2011;301:G623-G633.
34. Summerton JE. Morpholino, siRNA, and S-DNA compared: impact of structure and mechanism of action on off-target effects and sequence specificity. Curr Top Med Chem 2007;7:651-660.
35. Monga SP, Monga HK, Tan X, Mule K, Pediaditakis P, Michalopoulos GK. Beta-catenin antisense studies in embryonic liver cultures: role in proliferation, apoptosis, and lineage specification. Gastroenterology 2003;124:202-216.
36. Cui S, Capecci LM, Matthews RP. Disruption of planar cell polarity activity leads to developmental biliary defects. Dev Biol 2011;351:229-241.
37. Polat A, Emre MH. Effects of melatonin or acetylsalicylic acid on gastric oxidative stress after bile duct ligation in rats. J Gastroenterol 2006;41:433-439.
38. Dollins AB, Zhdanova IV, Wurtman RJ, Lynch HJ, Deng MH. Effect of inducing nocturnal serum melatonin concentrations in daytime on sleep, mood, body temperature, and performance. Proc Natl Acad Sci U S A 1994;91:1824-1828.
39. Glaser S, Onori P, Meng F, Franchitto A, Mancinelli R, Venter J, et al. Lack of the expression of the secretin-secretin receptor signaling axis exacerbates carbon tetrachloride-induced damage of large cholangiocytes. HEPATOLOGY 2011;54:A135.
40. Glaser S, Gaudio E, Onori P, Venter J, Chow B, Franchitto A, et al. Knockout of the gene for secretin inhibits biliary hyperplasia of large cholangiocytes in cholestatic mice by an autocrine mechanism. HEPATOLOGY 2009;50:1075.
41. Alvaro D, Invernizzi P, Onori P, Franchitto A, De Santis A, Crosignani A, et al. Estrogen receptors in cholangiocytes and the progression of primary biliary cirrhosis. J Hepatol 2004;41:905-912.

PLOS ONE

Distinct MicroRNAs Expression Profile in Primary Biliary Cirrhosis and Evaluation of miR 505-3p and miR197-3p as Novel Biomarkers

Masashi Ninomiya[1], Yasuteru Kondo[1]*, Ryo Funayama[2], Takeshi Nagashima[2], Takayuki Kogure[1], Eiji Kakazu[1], Osamu Kimura[1], Yoshiyuki Ueno[3], Keiko Nakayama[2], Tooru Shimosegawa[1]

1 Division of Gastroenterology, Tohoku University Hospital, Sendai, Japan, **2** Division of Cell Proliferation, Tohoku University School of Medicine, Sendai, Japan, **3** Department of Gastroenterology, Yamagata University Faculty of Medicine, Yamagata, Japan

Abstract

Background and Aims: MicroRNAs are small endogenous RNA molecules with specific expression patterns that can serve as biomarkers for numerous diseases. However, little is known about the expression profile of serum miRNAs in PBC.

Methods: First, we employed Illumina deep sequencing for the initial screening to indicate the read numbers of miRNA expression in 10 PBC, 5 CH-C, 5 CH-B patients and 5 healthy controls. Comparing the differentially expressed miRNAs in the 4 groups, analysis of variance was performed on the number of sequence reads to evaluate the statistical significance. Hierarchical clustering was performed using an R platform and we have found candidates for specific miRNAs in the PBC patients. Second, a quantitative reverse transcription PCR validation study was conducted in 10 samples in each group. The expression levels of the selected miRNAs were presented as fold-changes ($2^{-\Delta\Delta Ct}$). Finally, computer analysis was conducted to predict target genes and biological functions with MiRror 2.0 and DAVID v6.7.

Results: We obtained about 12 million 32-mer short RNA reads on average per sample and the mapping rates to miRBase were 16.60% and 81.66% to hg19. In the statistical significance testing, the expression levels of 81 miRNAs were found to be differentially expressed in the 4 groups. The heat map and hierarchical clustering demonstrated that the miRNA profiles from PBC clustered with those of CH-B, CH-C and healthy controls. Additionally, the circulating levels of hsa-miR-505-3p, 197-3p, and 500a-3p were significantly decreased in PBC compared with healthy controls and the expression levels of hsa-miR-505-3p, 139-5p and 197-3p were significantly reduced compared with the viral hepatitis group.

Conclusions: Our results indicate that sera from patients with PBC have a unique miRNA expression profile and that the down-regulated expression of hsa-miR-505-3p and miR-197-3p can serve as clinical biomarkers of PBC.

Citation: Ninomiya M, Kondo Y, Funayama R, Nagashima T, Kogure T, et al. (2013) Distinct MicroRNAs Expression Profile in Primary Biliary Cirrhosis and Evaluation of miR 505-3p and miR197-3p as Novel Biomarkers. PLoS ONE 8(6): e66086. doi:10.1371/journal.pone.0066086

Editor: Aftab A. Ansari, Emory University School of Medicine, United States of America

Received November 28, 2012; **Accepted** May 3, 2013; **Published** June 12, 2013

Funding: Financial support for this study was provided by Grant-in-Aid for Young Scientists (B) (23790765). The funders had no role in study design, data collection and analysis, decision to publish, or preparation of the manuscript.

Competing Interests: The authors have declared that no competing interests exist.

* E-mail: yasuteru@ebony.plala.or.jp

Introduction

MicroRNAs (miRNAs) are small endogenous RNA molecules of 19 to 24 nucleotides that control the translation and transcription of targeting mRNAs by base-pairing to the complementary sites [1] [2] [3] [4]. The expression of miRNAs in serum is reported to be stable, reproducible and consistent among individuals of the same species [5]. So far, specific expression patterns of serum miRNAs were identified as a fingerprint for numerous diseases and cancers [6] [5]. The serum miR-122 levels are elevated in patients with liver damage due to chronic hepatitis B (CH-B) and C infection (CH-C) [7] [8]. In addition, the miR-122 and miR-34a levels are positively correlated with the disease severity in CH-C and non-alcoholic fatty-liver disease [9]. However, there are some reports that miR-122 expression in healthy controls was significantly higher than that in patients with hepatitis C virus (HCV) infection [10]. Li et. al. described that 13 miRNAs were differentially expressed in hepatitis B virus (HBV) serum and that miR-25, miR-375 and let-7f could be used as biomarkers to separate a HBV-positive hepatocellular carcinoma (HCC) group from HBV-negative HCC [11]. However, little is known about the expression profile of miRNAs in autoimmune disease such as primary biliary cirrhosis (PBC).

PBC is female predominant, progressive autoimmune disease characterized by immune-mediated destruction of the intrahepatic bile ducts. The serological marker of PBC is the presence of anti-mitochondrial antibody (AMA) directed against the E2 subunit of the pyruvate dehydrogenase enzyme complexes located in the inner mitochondrial membrane [12] [13] [14]. The etiology of PBC is considered to be a combination of genetic predisposition and environmental triggers [15]. Particularly, concerning genetic predisposition, previous studies reported that common genetic variants at the HLA class II, IL12A, IL12RB2, STAT4, IRF5-

TNPO3 and IKZF3 had significant associations [16] [17] [18] [19] [20] [21]. Recently, genome-wide association study in Japanese population showed TNFSF15 and POU2AF1 as susceptibility loci [22]. Several GWAS data suggested the important contributions of several immune pathways to the development of PBC. However, the results have differed among the study groups [21]. The diagnosis of PBC is established based on the following criteria: (1) biochemical evidence of cholestasis; (2) the presence of AMA; and (3) histopathologic evidence of nonsuppurative cholangitis and destruction of the interlobular bile ducts [23]. Though diagnostic criteria have been determined, the eventual progression to biochemically and clinically apparent disease is unpredictable. Many patients are recognized at an earlier stage of disease and respond well to medical therapy, while some patients will require liver transplantation [24] [25]. To revolutionize the diagnosis, treatment and prognosis of PBC, new biomarkers seem to be feasible, and miRNAs are emerging as highly tissue-specific biomarkers with potential clinical applicability [26] [6].

In this study, we employed a strategy of using Illumina small-RNA sequencing for the initial screening followed by quantitative reverse transcription PCR (qRT-PCR) validation to analyze serum samples, which were arranged in multiple trial and testing sets. Additionally, computer analysis was conducted to predict target genes and biological functions from the differentially expressed miRNAs in PBC. The results demonstrate that the unique expression pattern of serum miRNAs can serve as a noninvasive biomarker for the diagnosis of PBC.

Results

Global analysis of miRNAs by deep sequencing

Circulating miRNAs were detected from human serum in 10 patients diagnosed with PBC and 15 non-PBC subjects with CH-B, CH-C and healthy controls, using Illumina GA IIx sequencing. Detailed clinical information is shown in table 1. We analyzed three samples by single-end deep sequencing on one lane and obtained about 12 million 32-mer short RNA reads on average per sample. After trimming the reads to exclude adaptor and tag sequences by using cutadapt, 9,245,752 high-quality reads per sample were subjected to analysis [27]. The mapping rates to miRBase were 16.60% on average and those to hg19 were 81.66% (Table 2).

miRNA expression profile in serum affected of PBC

We normalized the differential expression of miRNA count data using the trimmed mean of M values (TMM) normalization process and the number of individual miRNA reads was standardized by the total numbers of 1,000,000 reads in each sample [28]. Comparing the 4 groups (PBC, CH-C, CH-B and healthy control), the differential expression levels of miRNA were extracted using analysis of variance (ANOVA). 1594 miRNAs were detected by deep sequencing (Table S1). Due to the small number of miRNA detections, the statistical significance of 821 miRNAs could not be determined. The ANOVA was used to determine differentially expressed miRNAs and multiple comparisons procedure was applied to compare more than one pair of means at the same time. Therefore, in statistical significance testing in the remaining 773 miRNAs, the p-value by multiple comparisons was performed by calculating False discovery rate (FDR)<0.1. The expression levels of 81 miRNAs were found to be differentially expressed in the 4 groups. Although, several types of clinical data were shown to be different from PBC, M2 negative for PBC-8, ANA positive for PBC-10 or past HBV infection for PBC-6, the histologies of all samples were characterized by PBC of chronic, nonsuppurative cholangitis affecting the interlobular and septal ducts. The heat map and hierarchical clustering demonstrated that the miRNA profiles from PBC clustered with those of CH-B, CH-C and healthy controls (Figure 1). Of note, CH-B and healthy controls were not clearly distinguished.

In the result of Illumina sequencing, 3 miRNAs were up-regulated (>2-fold) in PBC patients, with hsa-miR-1273g-5p being most enriched. The relative levels of 6 dysregulated miRNAs were down-regulated (<0.5-fold), with hsa-miR-766-5p being the smallest (Table 3).

miRNA validation study

We used qRT-PCR to verify the data obtained from the Illumina sequencing. The relative expression levels from 9 differentially expressed miRNAs were analyzed with the TaqMan MicroRNA assay (Applied Biosystems) or miRCURY LNA microRNA PCR system (Exiqon). In addition to the 25 samples used for Illumina deep sequencing, 10 cases of miRNA expression in PBC, CH-C, CH-B and healthy controls were quantified (Table 4). The expression levels of selected miRNAs detected by qRT-PCR were normalized to spiked-in cel-miR-39 and presented as fold-changes ($2^{-\Delta\Delta Ct}$) above those of the CH-C-5. Among 9 miRNAs, the quantity of four miRNA expressions could be determined. The circulating levels of hsa-miR-505-3p, miR-197-3p and miR-500a-3p ($p<0.01$) were significantly decreased in PBC compared with healthy controls and the expression levels of hsa-miR-505-3p, miR-139-5p and miR-197-3p were significantly reduced compared with the viral hepatitis group (Figure 2). The quantities of miRNA expression by qRT-PCR were supported by the data of Illumina sequencing. Of note, for samples with only trace amounts, quantification of the reaction products after 30 cycles is uncertain. The quantity of 5 remaining miRNA expressions indicated the Ct values under 30 cycles even in the higher amount group or were undetected.

miRNA target genes and Gene ontology (GO) analysis

To determine possible target genes for the differentially expressed miRNAs, we searched the miRror 2.0 database for predicted miRNA targets in human. The ranking of miRror was according to the miRror Internal Score (miRIS). This score is a balance between (i) the proportions of predicting miRNA-target prediction databases (MDBs) out of all tested MDBs and (ii) the fraction of the potentially regulated genes from the entire input genes [29]. A total of 75 genes were predicted as targets for 9 differentially expressed miRNAs by Illumina sequencing of hsa-miR-1273g-5p, miR-33a-5p, miR-3960, miR-766-5p, miR-505, miR-30b, miR-139-5p, miR-197 and miR-500a in PBC serum (Table 5). Then, these 75 genes were submitted to Database for Annotation, Visualization and Integrated Discovery (DAVID) v6.7, which was used for the GO biological process categorization, Kyoto Encyclopedia of Genes and Genomes (KEGG) pathway and BIOCARTA pathway. The predicted target genes involved biological processes such as blood circulation (5.4%), circulatory system process (5.4%), positive regulation of I-kappaB kinase/NF-kappaB cascade (4.1%), regulation of phosphoprotein phosphatase activity (2.7%), cell volume homeostasis (2.7%), regulation of phosphatase activity (2.7%) and cellular amino acid derivative catabolic process (2.7%), some cellular components such as cytosol (13.5%), cell fraction (12.2%), membrane fraction (9.5%) and protein serine/threonine phosphatase complex (4.1%), and some molecular functions such as ion binding (33.8%), Cation binding (33.8%), metal ion binding (33.8%) and transition metal ion binding (25.7%) (Table S2). The functional annotation analysis of

Table 1. Clinical data for patients enrolled in Illumina sequencing analysis.

Patient	Sex	Age	Biopsy finding[a]	T-bil (mg/dl)	ALT (IU/l)	ALP (IU/l)	Albumin (g/dl)	PT-INR	ANA	AMA	M2 (index)	HBV-DNA (Log copies/ml)	HCV-RNA (LogIU/ml)	Past treatment[b]
PBC-1	M	60	II	0.5	36	404	3.8	1.00	-	1:80	128			URSO (−)
PBC-2	M	65	I	1.2	54	485	4.1	1.05	-	1:160	125			URSO (−)
PBC-3	F	61	II	1.2	38	478	4.0	0.97	-	1:20	89.5			URSO (−)
PBC-4	F	51	III	0.8	71	798	3.8	0.96	-	-	47.9			URSO (−)
PBC-5	F	62	II	0.6	26	407	4.0	0.99	-	1:20	102			URSO (−)
PBC-6	F	61	I	0.6	38	527	4.2	0.91	-	-	111.4			URSO (−)
PBC-7	F	55	II	1.0	53	800	4.2	1.02	1:80	-	89.9			URSO (−)
PBC-8	F	52	II	0.9	28	525	3.7	0.94	1:80	-	-			URSO (−)
PBC-9	F	72	I	1.1	42	666	3.4	1.00	-	1:80	143.9			URSO (−)
PBC-10	F	64	I	0.7	38	513	4.0	0.88	>2561	1:80	79.4			URSO (−)
CH-C-1	M	57	2	0.6	22	240	4.4	0.91					5.4	IFN (+)
CH-C-2	F	55	3	1.5	73	403	4.0	1.06					5.1	IFN (+)
CH-C-3	F	61	1	1.1	12	179	4.2	1.11					5.2	IFN (+)
CH-C-4	F	49	2	0.8	42	261	3.6	1.05					6.3	IFN (−)
CH-C-5	F	53	2	0.8	27	257	4.0	0.93					6.9	IFN (+)
CH-B-1	F	35	1	0.7	585	283	4.1	1.03				9.1		NA (−)
CH-B-2	F	72	2	0.9	64	211	3.8	1.03				3.4		NA (−)
CH-B-3	F	38	2	0.8	283	268	3.1	0.99				8.8		NA (−)
CH-B-4	F	43	3	0.6	87	239	3.7	1.01				7.4		NA (−)
CH-B-5	M	47	1	0.6	40	156	4.1	1.12				5.9		NA (−)
Healthy-3	M	37		0.6	24	252	4.2	1.02						
Healthy-4	F	49		0.7	21	274	4.1	1.08						
Healthy-5	F	33		0.6	18	173	3.9	1.12						
Healthy-7	M	26		0.8	35	218	4.3	1.08						
Healthy-8	M	28		0.9	22	238	4.2	1.04						

[a]We used the Scheuer score in PBC and fibrosis score of histological activity index (HAI) in CH-B and CH-C [53] [54] [55].
[b]URSO is the abbreviation for ursodeoxycholic acid, IFN for interferon and NA for nucleos(t)ide analogue.
doi:10.1371/journal.pone.0066086.t001

Table 2. The number of small RNAs in serum detected by Illumina sequencing.

		Cutadapt		Mapping (miRBase)		Mapping (hg19)	
Sample	Total	No. of read	% read	No. of read	% read	No. of read	% read
PBC-1	9,996,912	5,912,672	59.14	582,682	9.85	5,195,131	87.86
PBC-2	17,103,184	8,147,153	47.64	837,575	10.28	6,484,515	79.59
PBC-3	11,731,105	9,001,730	76.73	873,985	9.71	5,414,933	60.15
PBC-4	12,785,162	10,700,147	83.69	1,463,341	13.68	8,227,422	76.89
PBC-5	14,732,479	9,138,080	62.03	1,125,157	12.31	7,317,178	80.07
PBC-6	12,139,379	7,256,738	59.78	1,274,462	17.56	5,612,279	77.34
PBC-7	12,895,734	10,107,477	78.38	1,067,578	10.56	7,826,537	77.43
PBC-8	18,786,941	11,711,844	62.34	967,802	8.26	8,323,607	71.07
PBC-9	11,852,431	8,980,873	75.77	1,141,912	12.71	7,593,581	84.55
PBC-10	18,224,562	12,752,337	69.97	756,930	5.94	8,912,212	69.89
CH-C-1	10,874,814	7,820,291	71.91	2,870,316	36.70	6,924,685	88.55
CH-C-2	10,242,500	8,138,815	79.46	3,250,159	39.93	6,976,754	85.72
CH-C-3	19,183,649	12,135,107	63.26	1,878,487	15.48	9,056,579	74.63
CH-C-4	18,750,568	15,952,136	85.08	1,877,654	11.77	14,829,719	92.96
CH-C-5	12,702,304	10,306,186	81.14	1,592,422	15.45	9,269,394	89.94
CH-B-1	5,861,013	4,732,185	80.74	1,126,751	23.81	3,708,378	78.37
CH-B-2	7,164,871	5,937,732	82.87	1,213,392	20.44	5,076,436	85.49
CH-B-3	7,029,349	6,357,274	90.44	858,562	13.51	5,378,310	84.60
CH-B-4	8,077,025	6,788,987	84.05	1,581,475	23.29	6,142,836	90.48
CH-B-5	10,255,895	9,101,104	88.74	1,952,400	21.45	7,687,217	84.46
Healthy-3	11,111,254	7,843,011	70.59	1,248,499	15.92	6,778,655	86.43
Healthy-4	12,449,813	10,690,833	85.87	2,410,128	22.54	9,204,163	86.09
Healthy-5	13,597,339	8,914,365	65.56	2,214,635	24.84	6,571,819	73.72
Healthy-7	11,351,494	9,825,442	86.56	1,880,266	19.14	8,618,696	87.72
Healthy-8	14,349,933	12,891,294	89.84	2,320,100	18.00	11,618,231	90.12
Total	313,249,710	231,143,813	73.79	38,366,670	16.60	188,749,267	81.66

doi:10.1371/journal.pone.0066086.t002

BIOCARTA showed that the genes of catenin (cadherin-associated protein), alpha 1 and similar to breast cancer anti-estrogen resistance 1 predicted target genes of the listed miRNAs, and played a role in cell-to-cell adhesion signaling pathway (Figure S1). The KEGG pathway indicated that the genes of baculoviral IAP repeat-containing 2, protein phosphatase 3 catalytic subunit beta isoform and tumor necrosis factor ligand superfamily member 10 were related to apoptosis (Figure S2).

Discussion

MiRNA changes in the liver have been reported in diseases such as HCC or chronic viral hepatitis. However, there is only limited information about their detection in blood and their correlations in PBC patients. The current study provides the first evidence that PBC is associated with altered miRNA expression. We have demonstrated that a number of miRNAs, especially hsa-miR-505-3p and miR-197-3p, were significantly differentially expressed in patients with PBC, leading to a unique miRNA expression profile in the diseased liver. Recently, many studies have examined several PBC associations with genes and there have been significant differences in the genetic risk loci reported [21] [30]. Therefore more carefully constructed studies will be needed to clarify, the pathogenesis of PBC, and the study of these differentially expressed miRNAs could serve in identifying biomarkers or lead to a better understanding of the underlying molecular mechanism that perpetuates PBC.

In our study, miRNA Illumina deep sequencing was first used to screen 10 PBC patients' sera. We were able to match the sample's sex because of particular importance for X-linked miRNA [31]. Then, qRT-PCR was used to confirm the result of deep sequencing.

Quantitative differential expression analysis identified a 81-miRNA signature distinguishing PBC, CH-C, CH-B and healthy controls. A hierarchical clustering analysis was performed utilizing the 81-miRNAs and their patterns separated the PBC from viral hepatitis and healthy controls. In addition, there were three subgroups (PBC-1,2,4,5, PBC-3,6,10 and PBC-7,8,9) in the PBC cluster. When comparing the subgroups, the PBC-3, 6,10 group showed an expression pattern that differed from those of the other two subgroups. As for the clinical background, PBC-6 patient that had been infected with hepatitis B virus were HBsAg negative and anti-HBc and anti-HBs positive, and PBC-10 patient had positive antinuclear antibodies (ANA) titers of 1:2560 or greater, while other patients had no serological evidence of HBV infection and no positive ANA titers of 1:160 or greater. However, there was no clear difference between the three subgroups in terms of the clinical stage. At present, there is no conclusive proof whether